COGEAR

MODULE 2d:

Instrument evaluation, site selection and installation of permanent instrumentation

Del. No.: 2d.1.1 & Del. No.: 2d.1.2

and

Non-seismic short-term earthquake precursors

Del. No.: 2d.2.1

Authors: Álvarez-Rubio S., Fäh D., Abdelfettah Y., Balderer W., Leuenberger F., Kästli P., Schill E., Surbeck H., Tanner R., Zweifel P.

Swiss Seismological Service

SED/COGEAR/R/008/20110907
September, 8 2011

ETH
Eidgenössische Technische Hochschule Zürich
Swiss Federal Institute of Technology Zurich

SED
Schweizerischer Erdbebendienst
Swiss Seismological Service

Non-seismic short-term earthquake precursors

Project COGEAR

Coupled seismogenic geohazards in Alpine regions

Deliverable for
COGEAR Module 2d
SwissExperiment WP4.6

Sonia Álvarez-Rubio, Donat Fäh, Yassine Abdelfettah, Werner Balderer, F. Leuenberger, Philipp Kästli, Eva Schill, Heinz Surbeck, Robert Tanner, Peter Zweifel

Report

Swiss Seismological Service

ETH Zürich

September, 2011

SED/COGEAR/R/008/20110907

CONTENTS

1 Introduction

The goal of earthquake prediction is to warn of potentially damaging earthquakes early enough to allow appropriate response to minimize disaster loss of life and property, and therefore contribute to earthquake risk mitigation. During the last decades it has been found that sometimes geophysical and geochemical changes can precede the occurrence of intermediate and large earthquakes. Such short-term precursors are anomalous events or processes of different nature, seismological, geodetic, hydrogeological, geochemical, electromagnetic (EM), and so forth, that may precede an earthquake. Short-term prediction involves the monitoring of different processes that occur in the vicinity of a seismically prone region. The target is to study the occurrence pattern of these potential precursors and to analyze their dependence to the seismic activity taking place over long time periods as well as their natural changes due to different processes in nature. It is also a key issue to acquire quantitative knowledge of the physical mechanisms to which the earthquake precursors are linked in order to propose physical models to explain their occurrence or absence. Other scientific applications such as multi-parametric modeling of the structure under survey have to be addressed as well.

The large majority of earthquake precursory phenomena that have been studied and reported in the literature are related to the spatial extent and occurrence or absence of seismic activity, duration and intensity of activity, or amplitude signal/noise ratio among many others. Some models have been developed that provide plausible physical explanations but they are still stated in terms of many parameters that are often poorly resolved. One of the difficulties of detecting short-term precursors is that the processes that cause earthquakes occur at depth and therefore these phenomena are difficult to monitor. Selection of the instrumentation and sites for installation are key issues that pose many difficulties. Such monitoring needs to be long-term and continuous. Moreover, it is important to analyze and correlate data recorded with dense multi-sensor systems.

In a workpackage of project COGEAR (Coupled Seismogenic Geohazards in Alpine Regions) we took the first steps in Switzerland, toward the installation of permanent multi-sensor instrumentation for the detection of possible non-seismic short-term earthquake precursors. The topic has been addressed within Module 2d of the project. The study areas surveyed for this purpose are the Valais, with focus on parts of the Rhone, and the Visper and Matter valleys.

2 State of the art: non-seismic short-term earthquake precursory phenomena

In the last decades different studies have addressed short-term earthquake prediction by focusing on the observation of a very wide variety of physical phenomena that can precede the occurrence of earthquakes. These phenomena are called short-term earthquake precursors. They involve issues such as anomalous seismicity patterns, ground water level changes, gas emissions, geochemical changes in groundwater, seismo-electromagnetic phenomena, seismo-ionospheric coupling, surface deformations, animal behavior etc. These attempts of prediction have been reported in the literature showing the multi-disciplinary character. Examples like the anomalous magnetic fields recorded prior to the 1989 Loma Prieta earthquake by a magnetometer installed 7 Km away from the epicenter

(Fraser-Smith et al., 1990), the prediction of the 1975 M7.4 Haicheng event (Wang et al., 2006) in China, and many other phenomena reported so far (e.g. Cicerone et al., 2009), have boosted the support for scientific research in this field. Nevertheless, there is evidence in the literature of unsuccessful experiments (e.g. Bakun and Lindh, 1985). It should however be noted that in many cases these failures could be due to deficiencies of the monitoring experiment, not running in the best conditions related to the place and time of the seismic events.

Prestigious journals have encouraged earthquake prediction studies and surveys. Many successful reports have been presented; nevertheless others have also posed many question marks. Sevgi (2007) presents some of the key issues regarding earthquake prediction and in particular seismo-electromagnetic precursory-based earthquake predictors. The author reviews the criteria for the scientific process in earthquake prediction. He discusses reports where earthquake prediction is criticized in terms of scientific content (e.g. Geller, 1991). Earthquake prediction with precursors can be seen as being a difficult task: "*the earth is a complicated nonlinear system; the crust can be activated seismically with relatively small perturbation of the overall driving conditions; the complicated and non-linear seismology lacks a universally agreed physical mode…"* (Bleier and Freund, 2005). The author focuses on the idea that the earthquake precursor's studies should be well established in terms of scientific contents, problem complexity, signal excitation and propagation, causal relations with earthquakes, modeling of a sensor fusion problem, and public awareness and expectations. The paper is not to conclude whether detection of earthquake precursors is feasible or not, it is about the existence of scientific and societal grounds for funding large-scale prediction research programs. In this sense it is concluded that "*a scientific goal should be the understanding of fundamental physics of earthquakes and physics-based theory of the precursors (their causal correlation), not the reliable prediction of individual earthquakes…The efforts should be focused on the elimination from scientific journals of scientifically low-quality works, the exposure of works that contains errors and absurd statements made by scientifically unqualified publicity seekers".*

The International Association of Seismology and Physics of the Earth's Interior (IASPEI) has also pointed in this last direction. In order to raise the standard in earthquake prediction, it has fostered a panel of experts to evaluate the scientific rigor and quality of potential earthquake precursors drawing guidelines for precursory-based earthquake prediction. The IASPEI assessed the current state of the art of earthquake prediction research (Wyss and Booth, 1997) based on the following main criteria related to: "*(1) Physical model relating the precursor to the main shock, and the amplitude-distance variation of the anomaly associated with the precursor, including independent evidence for specially sensitive observation site, (2) the data, such as instrument positions and calibrations, associated environmental conditions, explanations of data gaps, data editing criteria, (3) anomaly definition (so that other data sets can be examined for anomalies), (4) the rules and reasons for associating a given anomaly with a given earthquake. There is also a requirement to evaluate the probability of the predicted earthquake to occur by chance, and to discuss the frequency of false alarms and failures to predict. The size of precursory anomalies should be compared with the size of any coseismic anomaly, and the relative sizes explained. A complete listing of significant earthquakes near the recording instrument is necessary so that any possible association with other shocks can be assessed".*

As results of this first revision, five precursors have been placed on the Preliminary List of Significant Precursors, out of the 40 evaluations made. The results of this first round of nominations have been published in a monograph (Wyss, 1991). It contains for each case the nomination material, the

anonymous reviewer`s comments, the IASPEI panel opinion, and the author´s reply. In Wyss and Booth (1997) it is explain that an inclusion of a precursor on the list does not mean that is a guarantee to be used for earthquake prediction, whereas the exclusion is not meant to tag the event as not capable anyway to be used for prediction. In fact, with this procedure the main purpose pursued is to stimulate discussion on the improvement of the evaluation of earthquake precursors and prediction. In fact, a second round of nominations for the IASPEI Preliminary List of Significant Precursors was proposed (Wyss, 1997). Among the precursors evaluated there were cases of non-seismic precursors such as radon changes in ground water and ground water level increase. In Table 1 the information of the two-non-seismic precursors is shown (Wakita et *al*., 1988, 1991; Roeloffs et *al*., 1997). These two cases have in common that they were recorded for a very long period.

Author	Precursor	Earthquake
H. Wakita, Y.Nakamura, K. Notsu, M. Nogutchi, and T.Asada	Radon concentration and temperature decrease in ground water (Ground water properties)	14 Jan. 1978, M 7.0 Izu-Oshima-kinkai
E. Roeloffs and E.G. Quilty	Ground water rise (Crustal deformation)	4 Aug. 1985, M 6.1 Kettleman Hills, California

Table 1. IASPEI Preliminary List of Significant Non-Seismic Precursors, March, 1994 (Wyss, 1997)

The recent works that aimed to the study of earthquake prediction, point out that it is a difficult topic to cope with, but not impossible. Seismology is a young science and the most relevant parameters, such as the stress level cannot be yet measured directly. There is need of conducting rigorous programs of earthquake prediction research that deal with fund raising and peer reviewing capable of catalogue scientific-based studies.

Cicerone et al. (2009) presents a very complete survey of published scientific literature concerning reported magnetic, electric and geochemical phenomena related with earthquake precursory studies. These precursory phenomena have been documented and characterized in terms of the earthquake surveyed, date, type of precursor, instrumentation, duration, amplitude, signal to noise ratio, and references. They have analyzed the dependence of the observation of each precursor on earthquake magnitude and investigated realistic physical models to enhance the understanding of the precursory earthquake signals. The precursory phenomena published (see Tables in Ciccerone et al, 2009) were observed under controlled credible and calibrated experiments. These phenomena correspond to electrical and magnetic fields, gas emissions, water level changes, temperature changes, surface deformations, seismicity. We will focus in this report on the investigation of the following non-seismic short-term precursors: magnetotelluric (electrical and magnetic changes) and geochemical (gas emissions, temperature changes, fluorescence emissions of thermal groundwater).

It is widely accepted in the literature that there are precursory and coseismic electromagnetic signals related to the occurrence of earthquakes. These phenomena are expected within a broad spectral range, from long-period variations to kHz frequencies: *ELF* (extremely-low-frequency), *VLF* (very-low-frequency), *ULF* (ultra-low-frequency). Reviews of the characteristics of electrical and magnetic fields linked to seismicity, electromagnetic data observation and analysis, and the physical mechanisms involved are presented in Park et al.(1993), Johnston, (1997), Hakayawa et al. (2000 and 2007), and Cicerone et al. (2009). Investigations of electromagnetic anomalous signals have been carried by

using ground-based and satellite-based instruments. In this work we will focus on the ground based techniques, a review of the most relevant results of the satellite techniques can be found in Cicerone et al. (2009), and Pulinets and Boyarchuk (2004). There are mainly two approaches to study electromagnetic effects expected on ground-based observations. The first is the direct observation of natural EM emissions due to seismogenic processes. The second type is indirect, through the observation of the characteristics that the signals from space exhibit in dependence of subsurface conductivity (Hayakawa et al., 2000 & 2007).

Since the 1990`s there have been many investigations carried out that suggest that ground-based electromagnetic measurements in the ULF range is a promising band for the search of earthquake precursory signals. One of the arguments that supports the use of ULF is that the skin-depth of ULF waves (it is the depth at which the wave energy is attenuated by a factor of 1/e), covers all possible earthquake source depths. Pioneering reliable ULF anomalies prior to earthquakes have been reported in the literature. Among others are the Loma Prieta event (USA, 1989 October 18, M=7.1) reported in Fraser-Smith et al. (1990) and Molchanov et al. (1992), the Spitak earthquake (Armenia, 1988 December 7, M=6.9) reported in Kopytengo et al. (1993) and Molchanov et al. (1992), the Guam event (Mariana Islands, 1993 August 8, M=8.0) reported in Hayakawa et al. (1996), and the Kobe earthquake (Japan, 1995 January 17, M=7.2) reported in Nagao et al. (2002). Other reported electromagnetic phenomena are presented in Table A1 (Cicerone et al., 2009). In the following we expose some of the main conclusions regarding these events.

Hayakawa (2007) presents results and discussions regarding seismogenic ULF emissions and its physical origin. The author states that there is evidence of ULF emissions prior to relatively large earthquakes, estimating a sensitive epicentral distance of 70-80 km for magnitude 6.0, and approximately 100 km for magnitude 7.0. It is also concluded that there is a temporal evolution of the ULF emissions for events with magnitude 6.0 and larger. Main sequential features observed are: a first peak one month to a few weeks before the event; a quiet period; finally a significant increase in amplitude few days before the earthquake. The amplitude of the emissions has been found to range between 0.1 nT to few nT. The most important frequency band remains an open issue, although there have been indications of the importance of periods around 100s. Different frequency bands were investigated. Different physical processes have been addressed to explain the origin of the emissions. The analysis of the data was always performed by simultaneously taking into account any man-made, geomagnetic and other existing noise sources.

Fraser-Smith et al. (1990) describe in detail the two electromagnetic monitoring systems running at the time when the Loma Prieta event occurred. The two systems provided complete coverage of magnetic field changes in a more than six decade frequency range from 0.01Hz to 32kHz. The ULF system was located at Corralitos, California, only 7 km away from the epicenter. The ELF/VLF system was located at the Stanford campus about 52 km from the epicenter. From the analysis of the data the authors concluded that the ELF/VLF data did not appear to show precursor activity, whereas the ULF data contained a number of anomalous features that could be identified as precursors. The lack of precursory information in the ELF/VLF data, was argued by the authors in terms of the depth of the event that might not have produced any of the surface electrical effects or changes, which presumably are required to launch ELF/VLF signals into the atmosphere. They also commented that former reports of VLF signals from earthquakes, involved deeper events than Loma Prieta, placed further away from the measurement systems. The distinctive and anomalous features regarding the ULF system highlighted in Fraser-Smith at al. (1990) are a narrow-band signal that appeared in the

range 0.05-0.2 Hz around September 12 and continued until the appearance of a second anomalous feature starting on October 5 and covering almost the entire ULF frequency range. An anomalous dip in the noise background was observed in the range 0.2-5 Hz starting one day before the earthquake, and an increase to high level of activity in the range 0.01-0.5 Hz starting approximately three hours before the earthquake (see Figure 1). In Bernardi et al. (1991) the anomalous ULF measurements recorded at Corralitos site prior to the Loma Prieta event is again studied. The authors expose that it was not found any reason to attribute these anomalies to any magnetic field fluctuation generated in the upper atmosphere or to movement of sensor caused by shocks preceding the quake. In Cicerone et al. (2009) the precursory magnetic fields associated to the Loma Prieta event is reported in terms of ULF ELF/VLF emissions. References and more details can be found in Cicerone et al. (2009).

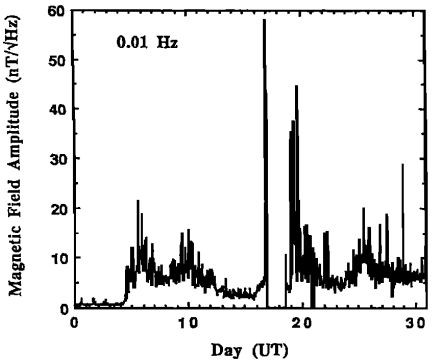

Fig.1 Variation of the Corralitos ULF 0.01 Hz. magnetic field measurements during October 1989. The Loma Prieta earthquake occured on October 18 and a power failure occurred almost immediately, whereupon the magnetic field measurements went to zero. The large peaks following the earthquake include many aftershocks as well as a magnetic storm that peaked October 20-21. The amplitudes can be converted to nT units (where 1 nT=1000 pT) by multiplying by $\sqrt{0.00732}$ or 0.0855. (Fraser-Smith et al., 1990).

The Loma Prieta event is an outstanding case to illustrate that the study of seismic precursors is a scientific field in continuous development that needs further high quality and long term observations due to its complex nature. In Thomas et al. (2009) the data analyzed in Fraser-Smith et al. (1990) and Bernardi et al. (1991) is studied again and the observation is expanded to a 21 month time window. They compared these data to 1.0 Hz magnetic field data collected from Japan and 0.0167 Hz data collected for the Fresno, California event. The authors conclude that the reported anomalous magnetic noise identified in Fraser-Smith et al. (1990) and Bernardi et . (1991), is not related to the Loma Prieta event, but is an artifact of sensor-system malfunctioning. Thomas et al. explain that the expectation of precursory phenomena can be due to the fact that, in the above mentioned papers, only a 2-month period of time around the occurrence of the event was investigated. Within this short period of time it is not seen that the Corralitos sensor was producing anomalous data long before the earthquake. It is concluded that successful earthquake prediction requires clearly identifiable indicators of the occurrence of an earthquake, and this must be reliably provided in a real-time setting.

Molchanov et al. (1992) and Kopytengo et al. (1993) address observations related to the Spitak earthquake. ULF magnetic emissions measured at two magnetic observatories in the Republic of Georgia (observatories Dusheti and Vardzia at distances around 129 and 85 km away from the epicentre of the event.) The measurements from Dusheti observatory analyzed are for the interval November 14, 1988 to March 5, 1989. The supplementary measurements used from Vardzia

correspond to the time window February-April 1989. Molchanov et al. (1992) compare the characteristics of the ULF emissions prior and after the occurrence of the Spitak event to those reported in Fraser-Smith et al. (1990) and Bernardi et al. (1991) regarding the Loma Prieta event. In this work it is observed that in both cases there are similarities between the recorded ULF magnetic field fluctuations. Among other conclusions the authors stated that: *(1) the intensity of ULF background activity started growing 3 to 5 days before the Spitak earthquake, whereas the corresponding increase in activity began 12 days before the Loma Prieta earthquake; (2) a substantial ULF emission burst was recorded at Dusheti starting 4 hours prior to the main shock, a similar large burst of ULF activity commenced 3 hours before the Loma Prieta event, and continued until the occurrence of the main shock; (3) ULF activity remained high for about two weeks after the Spitak earthquake, and for several months after the Loma Prieta earthquake; (4) ULF noise bursts were observed 1 to 6 hours before powerful aftershocks at Spitak during the period of enhanced activity, but there was no conclusive link between the ULF noise at Corralitos and the aftershocks (Loma Prieta event).* An important difference between the recordings related to the two earthquakes is the amplitude. This is explained in terms of the difference between the earthquake parameters of both events. In Figure 2 an example of the ULF emissions recorded at the Dusheti observatory after the Spitak event is shown.

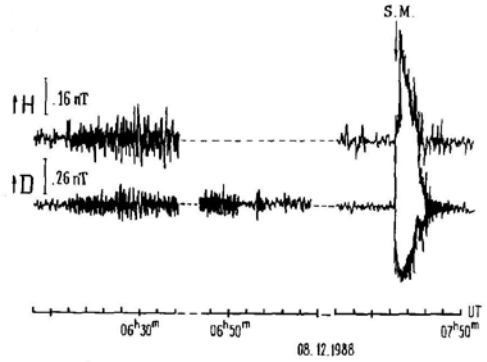

Fig. 2 Example of the intense ULF emissions at the Dusheti Observatory 06:24-06:55 UT which terminated 51 min before the strong aftershock at 07:46 h UT, 8 December 1988 near Spitak. The time of the aftershock is shown by the arrow indicated with S.M. (Kopytenko et al., 1993)

Kopytengo et al. (1993) analyzed more features of the ULF emissions recorded at Dusheti and Vardzia. They looked into the origin of the ULF signals, and concluded that the ULF field was not excited by magnetospheric-ionospheric sources. Moreover, they propose the sources of the emissions to be located in the Earth's crust.

Data covering a broadband spectrum, from ELF to HF, has been investigated in relation to the 1995 Kobe event (Nagao et al., 2002). Anomalous electromagnetic phenomena have been detected, that needed further research to exclude an atmospheric origin, and to clarify the possibility of a relation between pre-seismic electromagnetic signals and lightning, etc. In Hayakawa et al. (2000) monitoring of specific electromagnetic signals in the ULF range is discussed, focusing on the data processing and the physical origin of the disturbances. Different procedures are proposed to distinguish seismogenic signals from the background of space pulsations. The same techniques have been applied to observed data related to the Guam earthquake. A relevant result included in this work is the increasing variation of the long-period polarization ratio of Z/H one to two months before the earthquake (see Figure 3). This effect has also been identified in other studies.

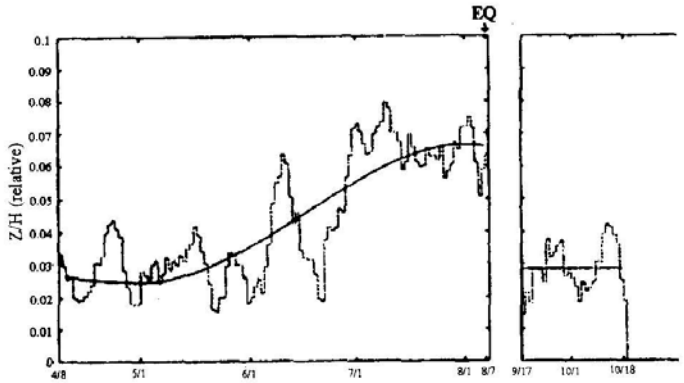

Fig. 3 Time sequence of the polarization ratio Z/H (5 day running average) for the Guam ULF emissions registered during the night (22-2 h LT). The time of the Guam earthquake of August 8, 1993 is marked by an arrow (Hayakawa et al., 2000).

Reported observed geochemical, thermal and hydrological anomalous signals preceding and during the occurrence of an earthquake cover a broad range of phenomena (Thomas, 1988; Wakita, 1996; Montgomery and Manga, 2003; Woith et al., 2003; Süer et al., 2008; Cicerone et al., 2009):

- Anomalies in the concentration of a variety of dissolved ions present in groundwater, changes in gas emissions from thermal and non-thermal wells, and discharge of odorous or flammable gases from the earth (monitoring of reactive gases such as CO_2, H_2S, CH_4, NH_4, etc., and inert gases He, Ne, Ar, Rn, N_2, etc).
- Groundwater level.
- Groundwater temperature change.
- Ground-gas geochemical anomalies
- Alteration of stream flow and water levels in wells.

A variety of mechanisms and models have been proposed in the literature to explain all these pre and co-seismic observations. Relations between observed anomalies and occurrence of earthquakes have been analyzed including the distance between the phenomena, correlations between earthquake parameters and measurement of specific anomalies, the time between events, etc. Some interesting and outstanding geochemical monitoring experiments are the ones related to the events in Kobe (Japan, 1995 January 16, M=6.9) reported in Igarashi et al. (1995), in Izmit (Turkey, 1999 August 17, M=7.6) and Düzce (1999 November 12, M=7.1) reported in Woith et al. (2003), Balderer et al. (2002), Belin et al. (2002), and in Chi-Chi (Taiwan, 1999 September 21, M=7.3) reported in Song et al. (2003). Reported chemical phenomena are presented in Cicerone et al. (2009).

In Japan a network of groundwater radon monitoring systems has been operated for about 20 years (Igarashi et al., 1995). From November 1993 to December 1995, a monitoring campaign of a well-known groundwater system has been carried out in the southern part of Nishinomiya city. The observation well is 17m deep and is located about 30 Km northeast of the hypocenter location of the Kobe earthquake (see Figure 4). The radon monitoring system worked correctly until the occurrence of the earthquake. The radon detection chamber fell down due to the strike of the earthquake, and no observations are available for several days after the event. Results showed an increase in radon concentration several months before the earthquake. Nine days before the earthquake this increase reached a peak of more than ten times the level of concentration at the start of the observations (Figure 4). Authors state that these changes are very likely to be precursory seismic phenomena.

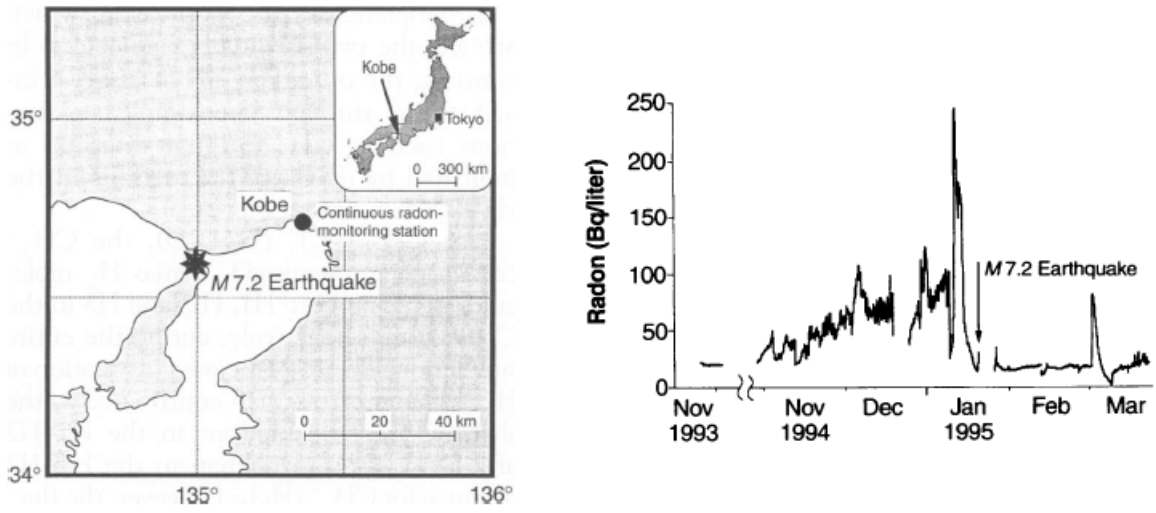

(a) **(b)**

Fig. 4 (a) Map of the continuous radon monitoring station and epicenter of the Kobe earthquake (from Japan. Meteorological Agency) **(b)** Radon concentration data at the well in the southern part of Nishinomiya city. Hyogo prefecture, Japan (Igarashi et al., 1995).

Another example of monitoring of groundwater properties is the case of the system deployed along the North Anatolian fault zone (Woith et al., 2003; Süer et al., 2008). Properties such as the water discharge, the water level, the water temperature, the specific electrical conductivity, pH, and radon have been monitored for several years, and especially during the Izmit and Düzce earthquakes. During this seismic active period (three months between the occurrences of both events), different geochemical stations were running located at different distances from the active faults. Some of the studies found anomalous signals at the most distant geochemical site. The electrical conductivity of mineral water from a flowing artesian well dropped co-seismically and post-seismically (Woith et al., 2003) (see Figure 5). The authors concluded that there is a response of the hydrogeological systems to earthquakes that seem to depend on the site rather than on the nature of the earthquake. They therefore highlighted the importance of a hydrogeological model for every monitoring site as to be able to interpret the response.

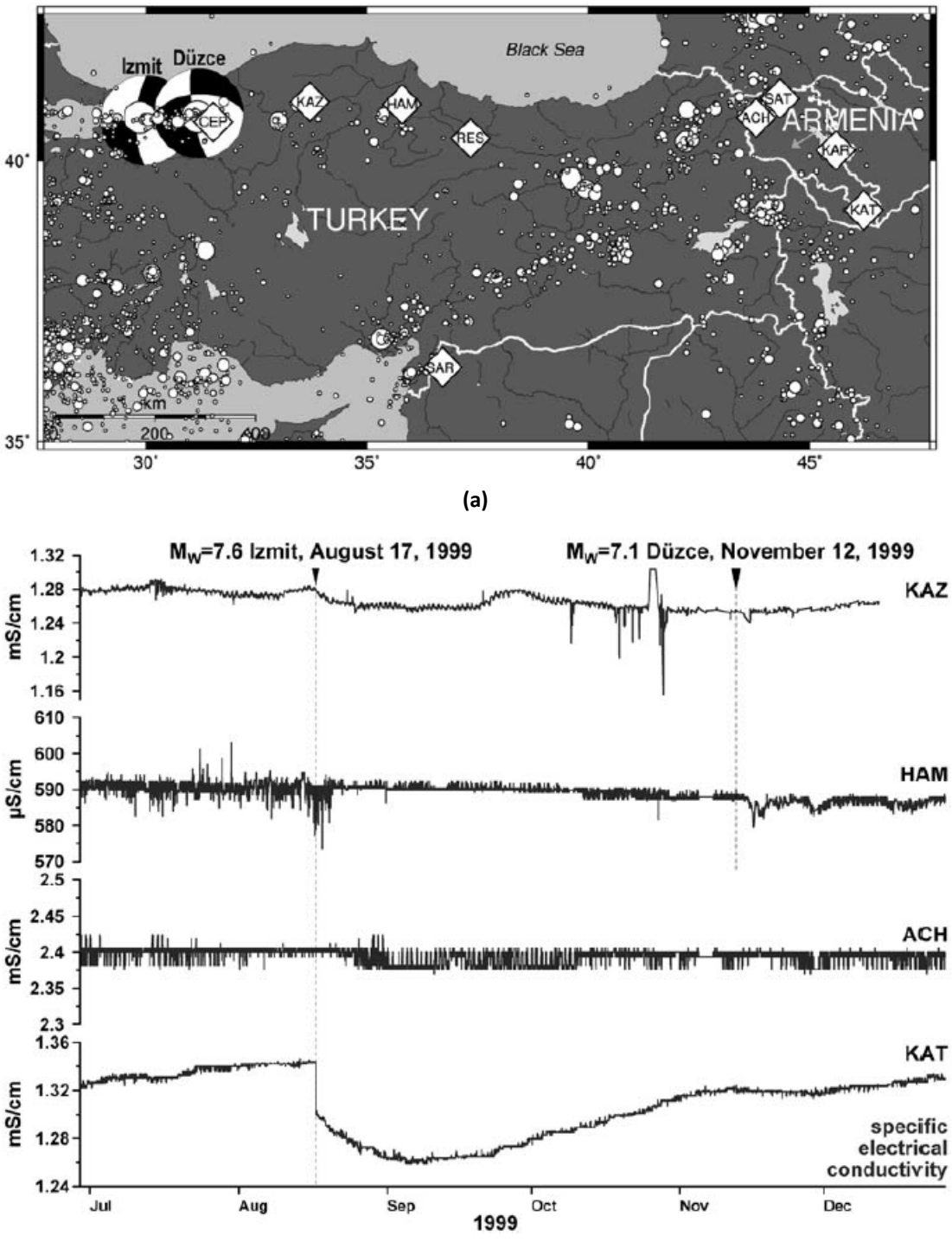

Fig. 5 (a) READINESS groundwater monitoring sites in Turkey and Armenia. Monitoring sites are indicated by *diamond symbols*. The location and focal mechanism of the M=7.6 Izmit earthquake of 17 August 1999 and the M=7.1 Düzce event of 12 November 1999 are also shown. During both events groundwater data were available from KAZ and HAM in Turkey, and from ACH and KAT in Armenia. *White circles* represent earthquakes above magnitude 4 according to the NEIC/PDE catalogue (Preliminary Determination of Epicentres provided by the National Earthquake Information Centre, USGS) between 1973 and 1999. **(b)** Time series of electrical conductivity monitored at four READINESS sites showing the different response to the Izmit and Düzce earthquakes.

Investigations have been performed for the detection of short-term geochemical and hydrological precursory phenomena linked to the destructive Chi-chi earthquake (21 September 1999, M=7.3) (e.g. Song et al., 2003). After the event commercialized bottled waters were collected (around 140 from December 1st, 1998 to 20 September 20, 1999). This water was taken from wells at Puli, Nantou County, in central Taiwan located about 10 Km northeast of the epicenter. The analyzed properties show sharp chemical anomalies and sudden increases in sulfate and nitrate ions. The concentrations increased after March 1999, as compared to the constant level measured since December 1998. They reached a peak in April 1999, dropped in July 1999, and gradually decreased until the earthquake. Large changes of groundwater levels were observed as well. The authors interpret these observations as stress/strain induced pressure changes in subsurface water systems and highlight that groundwater chemistry is a promising tool for monitoring earthquake processes.

3 Non-seismic earthquake precursors in Switzerland

3.1 Research and workplan

The milestones that summarize the main tasks in Module 2d of COGEAR project are:

- Recommendations on a surveying system for short-term non-seismic earthquake precursors in the Valais.
- Study of electromagnetic and geochemical signals. Installation of electromagnetic station and geochemical multi-sensor groundwater monitoring system.

We analyzed national and international projects related to the topic. We addressed the state of the art by revising the most relevant results and conclusions in the specialized literature (see section 2). The interdisciplinary character of the work, as well as the scientific and technical aspects of the project, emphasized the importance of networking between experts from different fields. Different institutions and scientific and technical programs have been contacted to encourage synergies and to discuss the first steps to be accomplished within the project. The main institutions are *SED-ETHZ* (Swiss Seismological Service, Switzerland), *ERDW ETHZ* (Departement Erdwissenschaften, Switzerland); *CHYN UNINE* (Centre d'Hydrogéologie et de Géothermie, Neuchâtel, Switzerland); *Nucfilm GmbH* (Switzerland); *SwissExperiment project CCES* (Switzerland); *EAWAG* (Das Wasserforschungs-Institut des ETH-Bereichs, Switzerland); *IGN* (Instituto Nacinal Geográfico, Spain); *CSIC* (Consejo Superior de Investigaciones Científicas, Spain); *School of Earth and Space Sciences, Peking University* (China); *Pushkov Institute of Terrestrial Magnetism, Ionosphere and Radio-waves Propagation, Russian Academy of Sciences* (Russia); *LVIV Centre of Institute of Space Research* (Ukraine); *EMSEV* (Inter Association Working Group on Electromagnetic Studies of Earthquake and Volcanoes); *Dublin Institute for Advanced Studies* (Ireland); Geothermal Exploration *ALPGEO* S.à.r.l (Switzerland); *INGV* (Instituto Nazionale di Geofisica e Vulcanologia, Italy); *Earthscope* (National Science Foundation, USA); *Metronix Messgeräte und Elektronik GmbH* (Germany); Tetraedre S.à.r.l (Switzerland); *Albillia S.à.r.l(Switzerland); Magson* (Germany); *Phoenix Geophysics Limited* (Canada); *SARAD GmbH* (Germany).

Several workshops and meetings have taken place during the first two years of the project. The partners shared their expertise, provided recommendations concerning:

- the instrumentation to be purchased (scientific goals, up to date technical description of the instruments available in the market, deployment of the equipment, data acquisition and transmission)
- the conditions and possibilities of test sites in the area of interest in Valais including parts of the Rhone, Visper and Matter valleys.

The site and instrument selection is for long-term operation of multi-sensor systems which is intended to run continuously. Some of the recommendations drafted are related to all the instruments, whereas others are specific to each type. As a first general directive, it has been stressed the need of multi-parametric analysis that can correlate all the different signals observed. In this way we can compile important information about the physical and chemical changes taking place at the site prior and/or during an event. The data can also be used to establish a dataset for the characterization of the hydrogeological, geochemical and dynamical regime of the region. Therefore sites should be spatially close enough to each other and within the area of research. The accessibility of the site is also a key point. The instrumentation is designed to be part of a long-term monitoring system that will be stepwise increased within the region according to the progress of the investigations. The maintenance in terms of equipment, data transmission and handling should be minimized. Fully automatic real-time systems are needed. As to fulfill the majority of these conditions candidates for test sites have been those already equipped with permanent seismic stations, power supply and online data transmission (internet connection).

3.2 Selection of geochemical and electromagnetic monitoring systems

The observation of geochemical earthquake precursory signals is carried out by the installation of two different monitoring systems that have been assembled for data logging and online real time streaming (see Figures 6 and 7).

For monitoring fluorescence spectral analysis of water we have chosen the *GGUN-FL30* field fluorometer designed in CHYN-UNINE and commercialized by Albillia S.à.r.l (see Figure 6). It has been used in the field for surveillance of natural and artificial flurorescent tracers and water turbidity, conductivity and temperature by CHYN (Schnegg, 2003; Flynn et al., 2006). Therefore it has been fully tested under real field conditions by groundwater professionals. Moreover, it fulfills the need for automatic and real-time on-line monitoring of dye tracer concentrations, water turbidity, temperature, pressure and conductivity.

Fig. 6 The GGUN-FL30 flow-through field fluorometer

Geochemical and physical variations in spring waters (gas emissions, changes of water level, etc.), are monitored by a multi-sensor instrument. It is the Nucfilm M_54 (Nucfilm GmbH) (see Figure 7). It is a customized solution built up to fit specific requirements of data recording and the site of installation. The concept has been previously tested in similar environments for different purposes by Surbeck et al. (2006). Further technical details are discussed in section 4.1.

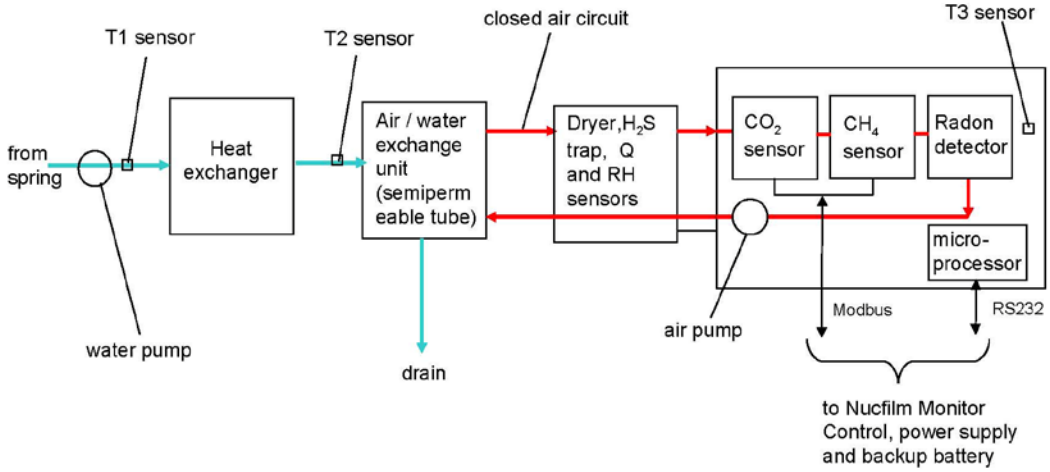

Fig. 7 Schematic overview of Nucfilm M_54 Radon, CO_2 and CH_4 monitor

The above presented instruments have been assembled to make an autonomous operational system. The data storing and transmission is operated by the datalogger TRCM-5 developed by Tetraedre S.â.r.l. The TRMC-5 has a number of I/O capabilities resulting in numerous possible configurations (see Figure 8). The ELAB-SED has adapted the device to the needs of the full geochemical monitoring system (Figure 9).

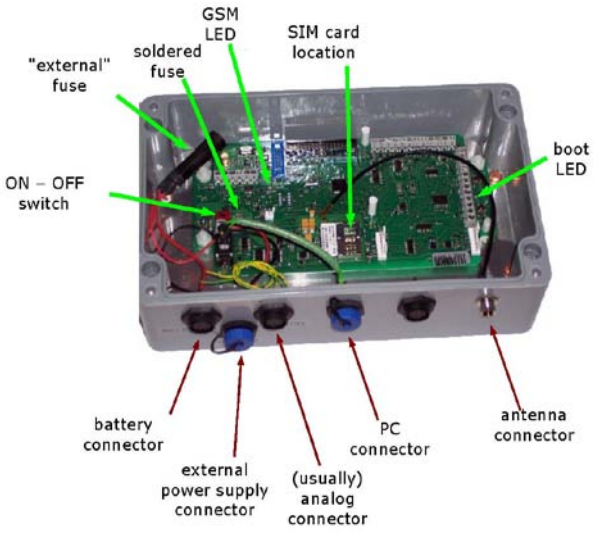

Fig. 8 Main elements of the TRMC-5 as provided by Tetraedre S.à.r.l

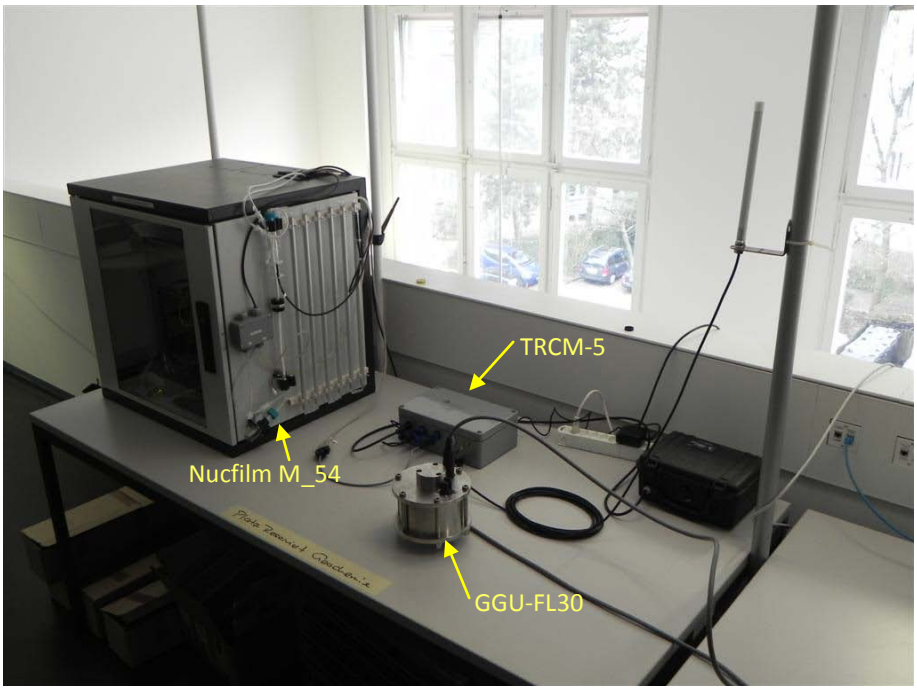

Fig. 9 Test at ELAB-SED of the full geochemical multi-sensor monitoring system: Nucfilm M_54 geochemical multi-sensor instrumentation; GGU-FL30 fluorometer, TRCM-5 datalogger; data transmission system.

The monitoring of electromagnetic precursory phenomena will be performed with the installation of magnetotelluric (MT) instrumentation (see Figure 10). In a first stage, only the three magnetic components will be recorded due to the fact that requirements of the installation of the electric sensors do not fit the requirements that are optimum for the project (see section 4.3). According to the feedback from the MT experts, our choice is to equip the sites with high quality magnetic coils rather than other sensors such as fluxgates. The main reason is that according to the skin depth

formula of electromagnetic waves and the resistivity range of the region, the coils are the ones that give best sensitivity to the top first kilometers where changes of conductivity induced by stress are expected. The full magnetic instrumentation (coils, datalogger) was provided by Metronix Messgeräte und Elektronik GmbH. The different induction coil magnetometers cover a wide frequency range from 0.0001Hz up to 50 KHz. Despite their wide bandwidth, they show an outstanding low-noise characteristics, extremely low temperature drift of input offset voltage and offset current and a stable transfer function over temperature and time. The system has an integrated calibration that eases the performance of online calibration or test of the magnetometer´s function. This instrumentation has largely been tested and used for different scientific goals (eg. Geiermann and Schill, 2010)

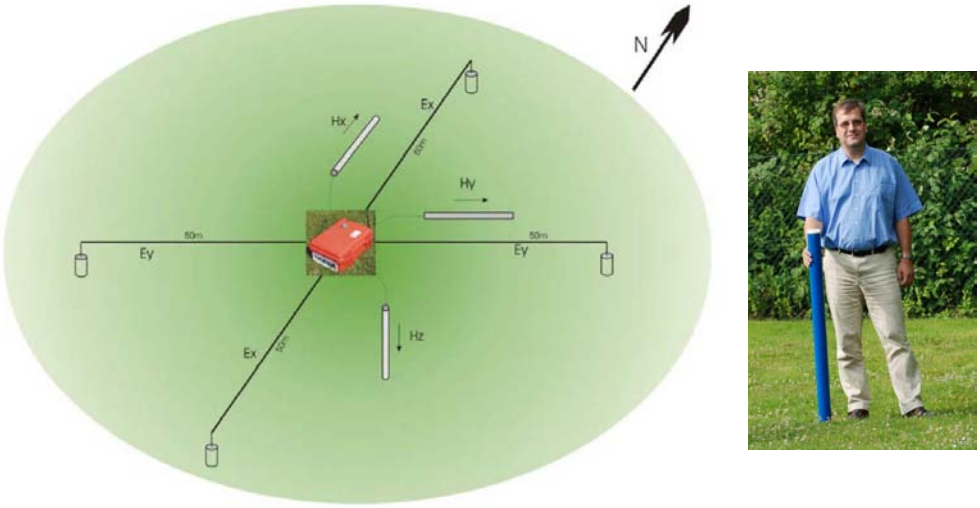

Fig. 10 Disposition of a full MT instrument on the field and details of induction coil magnetometer. Often, the electrical E_X and magnetic H_X components are pointed to the North, E_Y and H_Y to the East and H_Z down earth (figures from Metronix Messgeräte und Elektronik GmbH)

3.3 Site selection

The geochemical multi-sensor equipment has been planned to be installed to monitor changes in thermal ground water. Special care has to be taken to the presence of superficial ground waters at the spring water site that could highly influence the site. The selection of these sites is not easy in Switzerland because most of the springs are used, and therefore the pumping taken place can "shadow" the possible effects of earthquakes on the geochemical parameters measured. The possibility to see the Earth tides in the recording can be used as a good criterion during the selection of the site. Another decisive factor is the water temperature. This parameter should be high enough to guarantee that the depth of the source of the water analyzed is within the range of the depth of the seismic activity in the region.

The first site selected for the installation of the geochemical multi-sensor instrument, as well as, the fluorometer is the TQB1 natural spring located at Brigerbad which is a well known hot springs in Valais (see Figure 11). This site has been investigated by W. Balderer and H. Surbeck for a long time. The TBQ1 spring has been exploited, on a seasonal basis, for the facilities of the spa. In the last two years a geothermal project was conducted to seek new sources of thermal waters. At present, the

drillings have terminated and due to the positive results of them, the TBQ1 was available and we installed the geochemical equipment and fluorometer.

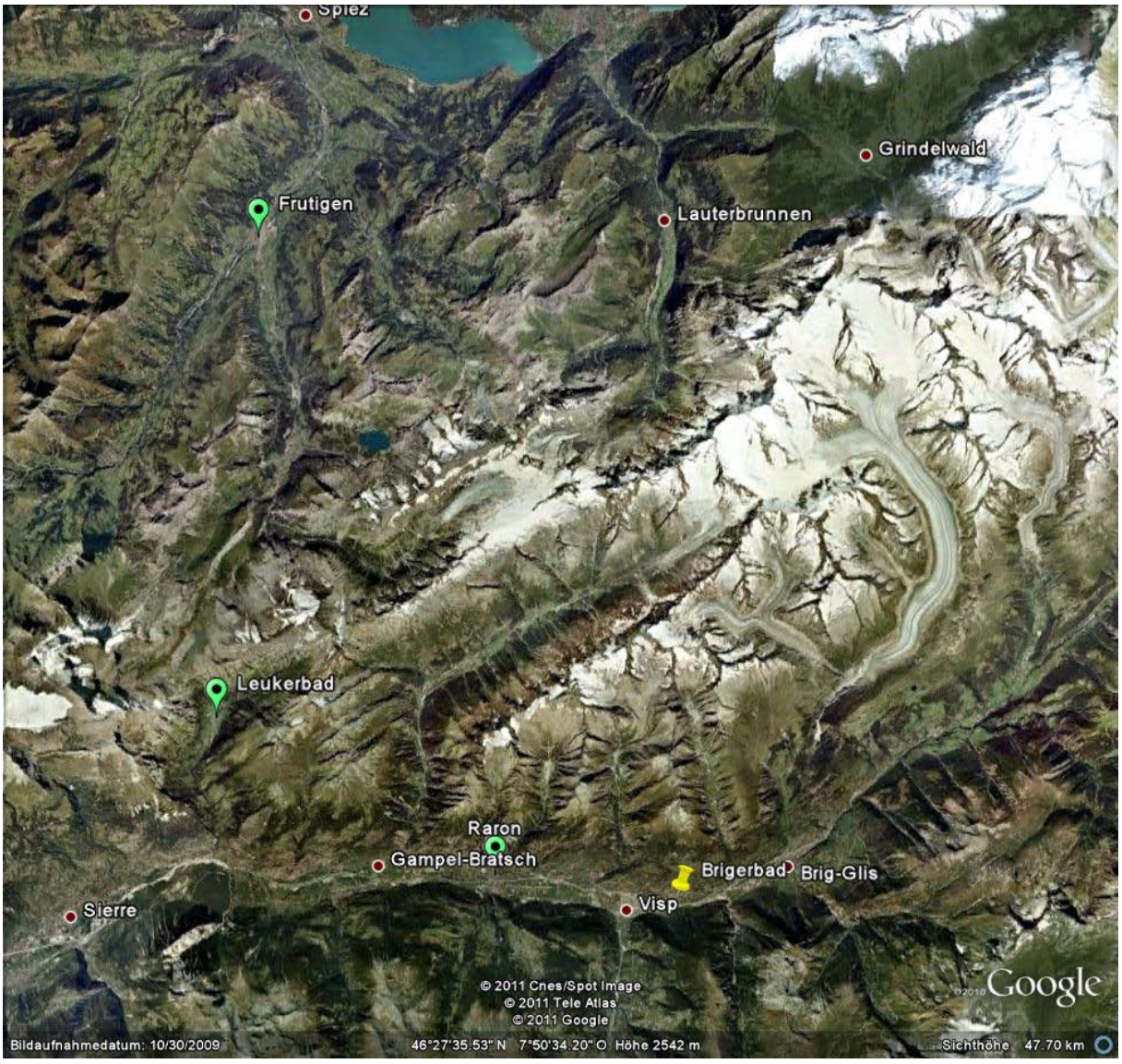

Fig. 11 Location of possible geochemical sites; Yellow pushpin: first selected site; Green paddle: further potential sites under discussion.

Other sites are investigated as a second potential site for geochemical investigations (see Figure 11). Two sites that were investigated are linked to the Lötschberg tunnel. At Tropenhaus in Frutigen, Canton Bern, they are using water drained in the northern part of the tunnel. The temperature is around 20 C and the discharge about 100 l/s. According to the information on internet, site water is drained from limestone of the Doldenhorn-formation. At the fish-farm Valperca in Raron, Canton Valais, the water used is drained in the southern part of the Lötschberg tunnel. The temperature is around 20 C. According to the first inquiries the waters drained to the north of the tunnel seem to be free flowing so there would be no problem of pumping effects. The third site under inspection is Leukerbad, Canton Valais. The springs within the area are free flowing and do not undergo pumping

of water. There are several unused springs but even a spring used for wellness purposes would be, in our opinion, suitable for the installation of the geochemical instrumentation.
For the installation of a magnetotelluric station there are many disturbing factors such as, DC train railways and other anthropogenic sources that make the selection of sites for installation of electromagnetic instrumentation a difficult task to accomplish. These conditions are especially critical in densely populated areas such as the area of study. Inhabited areas and power lines should be kept at least few Km away. Distance to railways lines should be even larger, particularly to DC trains (the distance depends on the ground conductivity). In the Swiss Alps the main cultural noise source is caused by the activity related to the electrical power production. During the night, an additional noise source can be generated by the pumps used to fill the water reservoirs. Therefore it was decided to do a first selection of sites in order to carry out a magnetotelluric (MT) test campaign to assess the local conditions. It is difficult to choose sites to perform MT soundings and it requires experience. Therefore the test campaign was carried out by SED-ETHZ and the MT experts of CHYN-UNINE (see section 4.3). The data recorded has been analyzed to decide on the suitability of the sites for the installation of a long-term electromagnetic instrumentation.
A first set of sites to perform the MT work field tests was chosen from the ones mentioned in a MT campaign carried out on 1996 in the penninic Alps (Schnegg, 1998). In this work there is useful information to locate suitable sites. Several problems were stressed by the author, that could affect the data quality. Among the largest problems were the DC railways, specifically 30 Km around the Martigny area and the Bern-Valais border region. The author noticed that the northern side of the Rhone Valley was perturbed by DC trains ending in Lenk (BE). Similarly, sites located in the main valley, as well as along the Simplon road were heavily perturbed (powerlines, industry). On the western side, the Martigny-Chatelard DC train was too close to the sites of Val Ferret and prevented reliable results. The AC trains did not significantly perturb the soundings, except in the area of Simplon pass, the Lötschental and in the Rhone Valley. This was not the case in the mountains which constitute the border between the cantons of Valais and Bern. Otherwise, all other sites located in the Penninic Alps were found convenient. Table 2 lists all the MT sites studied in Schnegg (1998). A “Y” letter is written in the last column when the site was improper for inclusion in the data inversion.

Nr	Date	Abbr.	East m	North m	X rel. km	Y rel. km	Elevation m	Site name	Data avail. gds/both	Telluric azimuth	EM perturbed
1	08.06.88	ZIN	614'890	106'780	48.27	23.84	1723	Zinal	both	0	
2	09.06.88	BOS	619'960	115'370	56.96	28.74	1901	Turtmanntal	both	0	
3	10.06.88	LOE	632'190	142'770	81.25	46.36	1788	Loetschental	-	0	Y
4	20.09.88	MOY	610'790	105'890	44.28	25.12	2350	Moiry	both	0	
5	21.09.88	MAU	592'800	92'910	22.21	22.87	2420	Mauvoisin	gds	0	
6	22.09.88	CLE	589'990	109'060	27.85	38.26	1989	Cleuson	both	0	
7	02.08.90	TRI	594'900	107'745	31.44	34.67	2282	Combe de la Rosette	both	0	
8	02.08.90	LOU	605'397	113'295	43.31	34.23	2700	Louché	both	0	
9	02.08.90	DON	594'620	130'030	42.34	54.11	2400	Donin	-	0	Y
10	06.08.91	ARO	600'770	96'000	30.66	21.56	2500	Montagne d'Arolla	both	0	
11	06.09.91	OLE	590'100	100'920	23.88	31.16	2420	Louvie	both	0	
12	30.09.92	TOU	615'410	116'200	53.43	31.74	2507	Tsa du Touno	both	0	
13	30.09.92	LUS	600'680	105'000	35.08	29.40	2205	La Luesse	both	0	
14	06.09.93	COL	604'030	94'730	32.84	18.83	2070	Les Collons	both	0	
15	06.09.93	FER	608'790	99'880	39.54	20.91	1960	Ferpècle	both	0	
16	07.09.93	DIX	596'530	99'560	28.76	26.76	2400	Dixence	both	30	
17	07.09.93	NOU	600'710	107'100	36.15	31.20	2310	La Nouva	both	0	
18	06.09.94	VER	584'260	108'025	22.37	40.23	2140	Verbier	gds	34	
19	07.09.94	MAV	594'090	88'310	21.03	18.24	2015	Sud Mauvoisin	both	30	
20	09.09.94	PRA	574'790	88'760	4.54	28.28	1609	Prayon	gds	0	Y
21	09.09.94	SAL	574'720	92'500	6.35	31.55	1265	Saleina	gds	40	Y
22	05.09.95	ZER	618'260	94'630	45.12	11.63	2218	Zermatt	both	0	
23	05.09.95	TAS	629'340	100'210	57.50	10.92	2218	Täschalp	both	15	
24	06.09.95	BUR	631'290	124'280	71.23	30.79	1780	Bürchen	both	0	
25	06.09.95	GAS	629'650	113'440	64.39	22.23	1680	Gasenried	gds	0	
26	11.09.95	NAN	640'810	117'990	76.33	20.59	2250	Nanztal	both	0	
27	11.09.95	NES	642'520	122'780	80.20	23.88	2470	Nesseltal	both	0	
28	12.09.95	SIM	646'660	116'860	80.83	16.68	1600	Simplon	gds	0	Y
29	12.09.95	PFY	612'000	127'800	56.28	43.49	564	Pfyn	-	0	Y
30	04.06.96	MAS	601'000	116'800	41.25	39.46	1840	Mase	both	0	
31	04.06.96	REC	605'575	118'725	46.18	38.84	1580	Réchy	both	0	
32	09.10.96	THO	594'380	75'820	15.03	7.28	1095	Thoules	both	0	
33	09.10.96	BAR	589'280	80'050	12.73	13.49	1580	Barlia	both	0	
34	09.10.96	OYA	596'890	78'790	18.69	8.60	1538	Oyace	gds	0	
Origin & rotation an			585'000	62'000	30						

Table 2 MT sites studied in Schnegg (1998).”Y” means the site was found improper for inclusion in the data inversion

Combining all information gathered and the priorities of the work, the four following sites where selected for test measurements: VANNI, EMBD, SIMPL, Bürchen (see Table 3 and Figure 12).

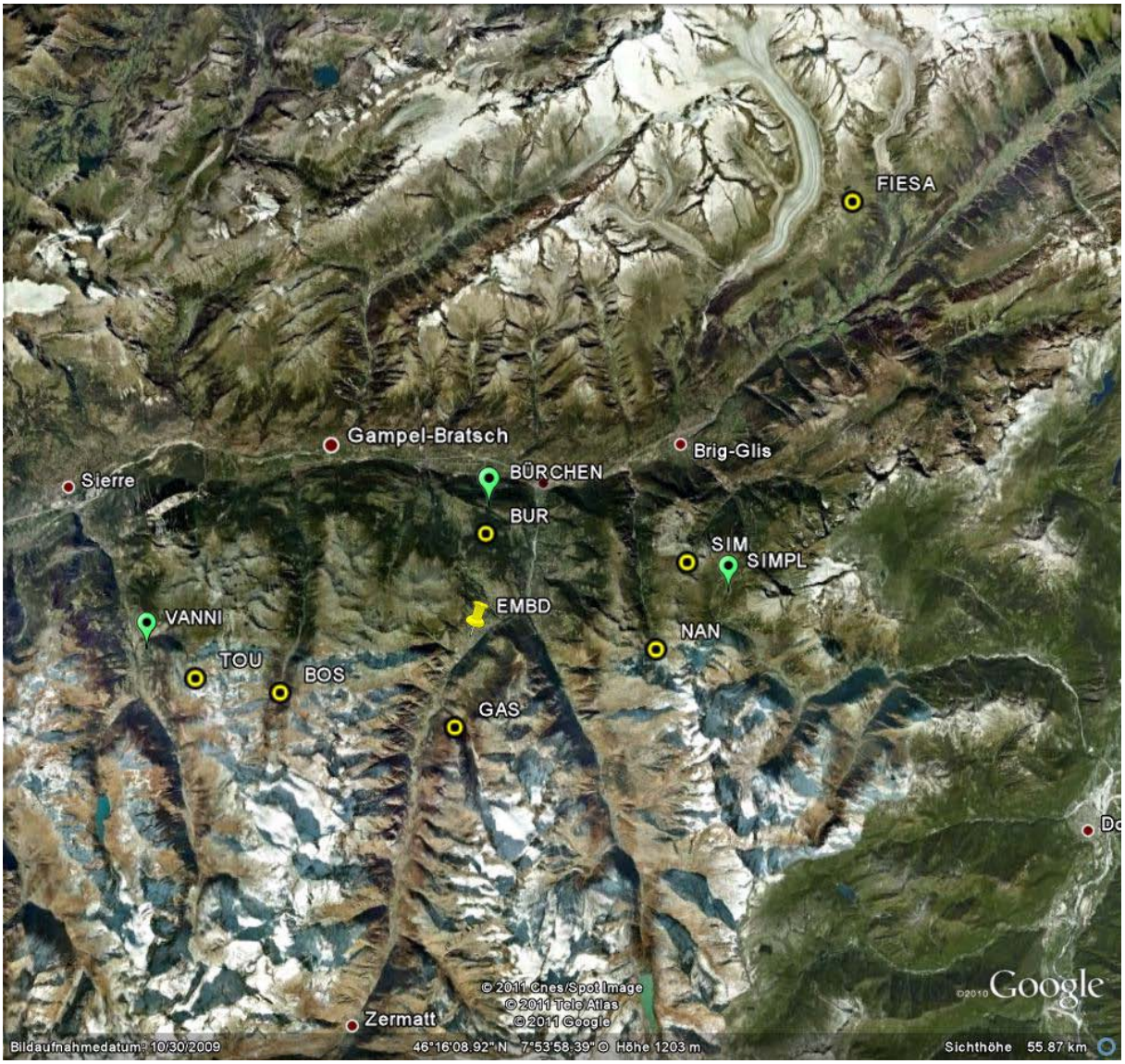

Fig. 12 Location of potential MT sites. All, except site BÜRCHEN, are equipped with seismic stations installed during project COGEAR. Green paddle: sites selected for the MT test work field. Yellow pinpush: first MT site. Coordinates are listed in Table 3

Code	Swiss Coordinates X	Y	Latitude	Longitude
VANNI	612204	117635	46.21005855	7.59677603
TOU	615410	116200	46.19708445	7.63826981
BOS	619960	115370	46.18949904	7.69717574
GAS	629650	113440	46.17178158	7.82256081
EMBD	630372	118417	46.21651992	7.83223205
BUR	631290	124280	46.26921846	7.84452054
NAN	640810	117990	46.2121276	7.96745596
SIM	642520	122780	46.25510973	7.99004903
SIMPL	644810	121074	46.23961509	8.0195813
FIESA	651631	142879	46.43526897	8.11042664
BÜRCHEN*	631336	125743	46.28237167	7.845211908

Table 3 Coordinates of the seismic stations of COGEAR project.* Open air site used for testing magnetic and electric instrumentation.

4 Non-seismic instrumentation in COGEAR

In this chapter specific reports of different experts are provided. These experts have been involved in the first steps towards the establishment of a non-seismic instrument network devoted to the monitoring of geochemical and magnetic signals.

4.1 Geochemical monitoring of dissolved gases

Dr. Heinz Surbeck, Nucfilm GmbH, Fineta 46, CH-1792 Cordast

4.1.1 Introduction

There have been numerous stories about strange spring behavior before, during or after an earthquake. Dramatic changes in discharge, gas bubbles or even flames above the water have been reported.

Most of these stories are anecdotal, but there has been quite a lot papers in scientific journals describing a change in dissolved gas concentration during a seismic event. Frequently one can find claims about radon concentration increases prior to a quake. A well-documented case seems to be a radon peak days before the great Kobe earthquake in 1995 (Igarashi, et al., 1995). A weak point of all these papers claiming to have seen precursors is that the measurements have been made in seismically very active zones like the Himalayas, Japan or California. Earthquakes are so frequent there that it is very difficult to attribute a radon peak to a distinct seismic event. It may be either really a precursor or simply a reaction to an earlier quake.

The COGEAR project now has paved the way for a serious study of possible correlations between dissolved gas concentration changes and earthquakes. Important seismic events (M > 4) are rare in the study area (greater Visp region) but the potential for strong ones is real. In addition there is a hot spring (Brigerbad) in this region. Hot springs react particularly well to changes in mixing ratios due to changes in strain patterns deep down. Hot springs are also less influenced by changes in atmospheric conditions than springs fed by near surface groundwater. Thus the main Brigerbad spring was equipped with a dissolved gas monitor built by Nucfilm GmbH. Radon CO2 and CH4 will be measured continuously with a temporal resolution of about an hour.

An alternative or additional site would be a nearby fish-farm that uses warm water collected in the new Lötschberg railway tunnel.

4.1.2 Description of the radon, CO_2 and CH_4 monitor (*Nucfilm M_54*)

The monitor Nucfilm M_54 measures radon, CO_2, and CH_4 gases by sensors placed in a closed air circuit coupled to the water to be measured by a semipermeable membrane.

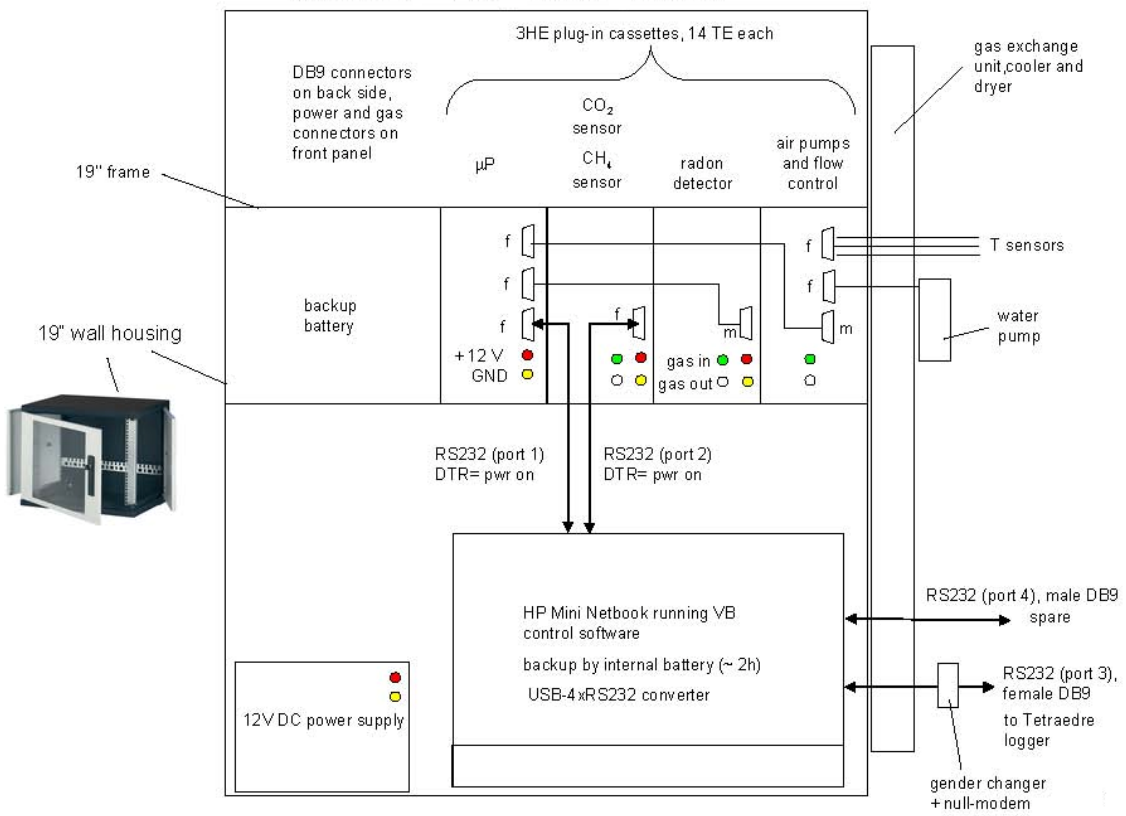

Fig. 13 Overview of the Nucfilm M_54 Radon, CO_2 and CO_4 monitor. Tetraedre logger is the datalogger chosen for data streaming

The radon sensor is a 20 ml Lucas-cell coupled to a photomultiplier. Alpha particles emitted by decaying radon and radon daughter products like Po-218 and Po-214 interact with the solid scintillator (ZnS:Ag) inside the Lucas-cell. The light pulses produced are seen by the photomultiplier and are counted. The count rate is then a measure for the radon concentration. The CO2 and CH4 sensor modules are dual beam non-dispersive IR-absorption instruments, tuned to the absorption bands of the respective gases. All three sensors work well up to a relative humidity of 99 % but would be damaged if there is condensation.

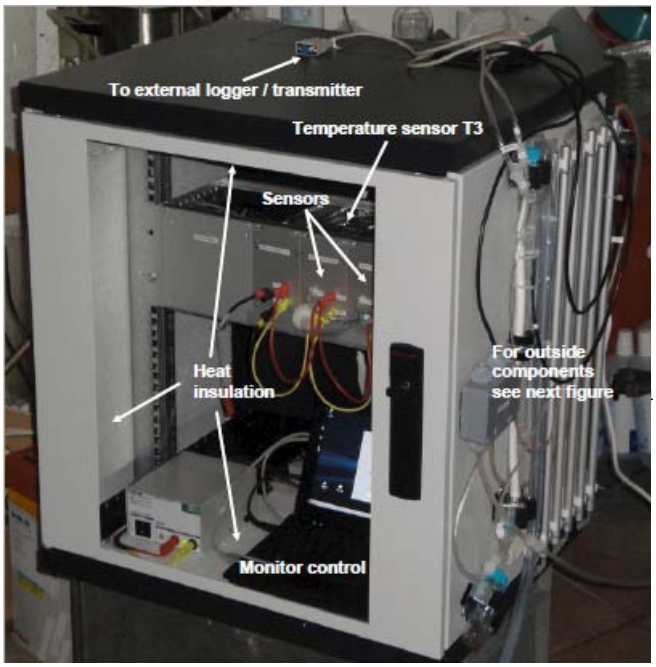

Fig. 14 *The Nucfilm M_54* monitor

Condensation is the main problem when measuring hot water. To avoid condensation the water temperature at the semipermeable membrane has to be slightly below the sensor temperature.
The water temperature of the Brigerbad spring can be as high as 50 C. This water has to be cooled down before it can be measured. Part of this cooling down will happen during transport from the spring to the monitor (~ 30 m tube). An additional cooling down to near room temperature will be made with a heat exchanger just in front of the monitor. The Brigerbad spring water is known to contain dissolved H2S. This gas can attack sensor components. Thus there is a H2S trap (iron filings) placed in the air circuit after the membrane tube.
A “Permapure” tube, see Figure 15 placed in the air circuit after the H2S trap will reduce humidity near to room air relative humidity. This type of tubes lets pass water vapor easily but is impermeable for radon; CO_2 and CH_4. As a last hurdle for water droplets to enter the sensor circuit there is a Teflon aerosol filter in front of the first sensor. Teflon filters don't let pass water. Heat dissipated by the electronics inside the partly heat insulated monitor case leads to a temperature inside the monitor well above the room temperature.
Water temperatures at the heat exchanger input and at the semipermeable membrane and the temperature inside the monitor case are measured. Relative humidity in the air circuit is measured too.
Temperature and humidity data are used to control water pump rates and air pump rates to avoid condensation. This control task is handled by a HP-Mini PC running a Visual Basic program. This PC also converts sensor readings to physical units and displays these data. The PC gets the sensor readings either from a microprocessor (counter, ADC) communicating with the PC over one of the 4 serial lines (radon counts, temperature, flow and relative humidity) or for the CO_2 and CH_4 values over a MODBUS connected to another serial line. Digital outputs of the microprocessor are used to control power for the pumps. Data updated once an hour are stored internally and are sent on request over a serial line to the SED equipment. There is a spare serial line where in the future additional sensors could be connected.

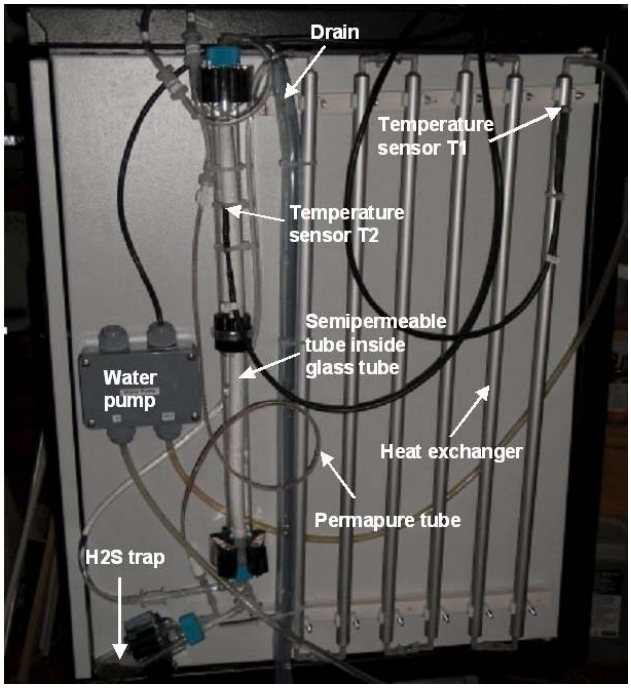

Fig. 15 Outside components of the *Nucfilm M_54*

4.1.3 Data specification

The data measured by the multi-sensor is updated once an hour, stored internally and sent on request to Tetraedre datalogger. The data is recorded in the following ASCII string

Y, 2011,M,1,D,21,H,16,N,57,RN,2105,CO2,31,CH4,12,T1,300,T2,200,T3,250,Q,220,RH,800,VC,112CR

Y=year, M=month, D=day, H=hour, N=minute, time zone :UTC
Dissolved gas concentrations:
Radon concentration (air circuit): [RN]= counts/h, conversion to Bq/l in water depends on temperature and flow rates (air pump and water pump). Conversion factor has been determined by Nucfilm during installation at real site.
CO_2 concentration (air circuit): $[CO_2]$= 0.01 Vol%, factory calibrated
CH_4 concentration (air circuit): $[CH_4]$ = 0.01 Vol%, factory calibrated
Diagnostic parameters:
Temperatures: $[T_i]$=0.1 C
Air flow: [Q]=ml/min
Relative humidity: [RH]=0.1%
Supply voltage: [VC]=0.1 V

4.2 Monitoring of fluorescence of outflowing thermal water

Dr. Werner Balderer, Dr. Fanny Leuenberger-West, Institute of Geology, ETH Zürich

The analysis of the Brigerbad thermal water has been started by the Geological Institute of ETH, and by the University of Neuchatel in relation to the geothermal exploration and related drilling. An initial preparatory sampling of thermal water from the natural out flowing Brigerbad spring was carried out in 2007. The daily samples of groundwater collected over a two-month period were analyzed by fluorescence spectroscopy (synchronous scanning method) over a wavelength range of 200 to 800 nm, with a difference between excitation and emission wave length of 20 nm. It was revealed that the variation of the intensity at 389 nm was characteristic also for the total integrated intensity in the interval of wavelengths from 300 to 600 nm. A monitoring device was designed with a fixed dedicated wavelength interval of 20 nm, 369 nm excitation wavelength and 389 nm wavelength from the emitted fluorescence signal (instead of using a much more expensive synchronous scanning instrument, which would scan the whole fluorescence spectra between 200 and 800 nm). Since 26.8.2009 such a special designed fluorometer is installed at the Brigerbad thermal spring. With this instrument the fluorescence is measured in 3 channels of different wavelengths. These channels are named according to the most prominent artificial tracer which wavelength is within the chosen interval:

Naphthionate: this interval of fluorescence spectra is most sensitive of humic acids.

Tinopal X: This interval of the fluorescence spectra is the most sensitive to tectonic caused perturbations of the water fluorescence, and is therefore the most premising for the perception of seismic precursor phenomena.

Uranine: This spectral interval is already at higher wavelengths than of interest for the observation of natural variations as seismic precursor signal. But it was remained in the fluorometer also as possibility to use this instrument for tests with the artificial tracer uranine and also for instrument calibration purposes.

As fourth channel also the *turbidity of the water* is monitored, because the turbidity influences the fluorescence measurements and is used therefore as internal correction parameter of the fluorometer itself (Schnegg, 1996). Additionally also the water temperature is measured at the same time intervals as the other parameters.

As an example in Figure 16, a short monitoring period of 1 hour is represented. The measurement of the specific wavelength domains of Tinipal X (green line), Naphthionate (blue line) and Uranine is represented. The interval between 2 measurements is 30 seconds. Within this record the Naphthionate spectral range shows the highest signals. Further interpretation of longer intervals of time will follow and especially the on-line transmission will enable more insights into the recorded processes.

4.2.1 Data specification

The measurement is in relative units. For the logging instrument there is a conceptual difficulty: The fluorometer CHYN is designed for the detection of artificial tracers as Uranin, Rhodamine Tinopal, at their specific wavelengths of excitation and emission. But as we are looking for natural fluorescence it is just to be described as “fluorescence intensity” in the uranine, rhodamine or tinopal channel. Also the wavelengths ranges have been modified to be more specific for the natural fluorescence changes we want to observe.

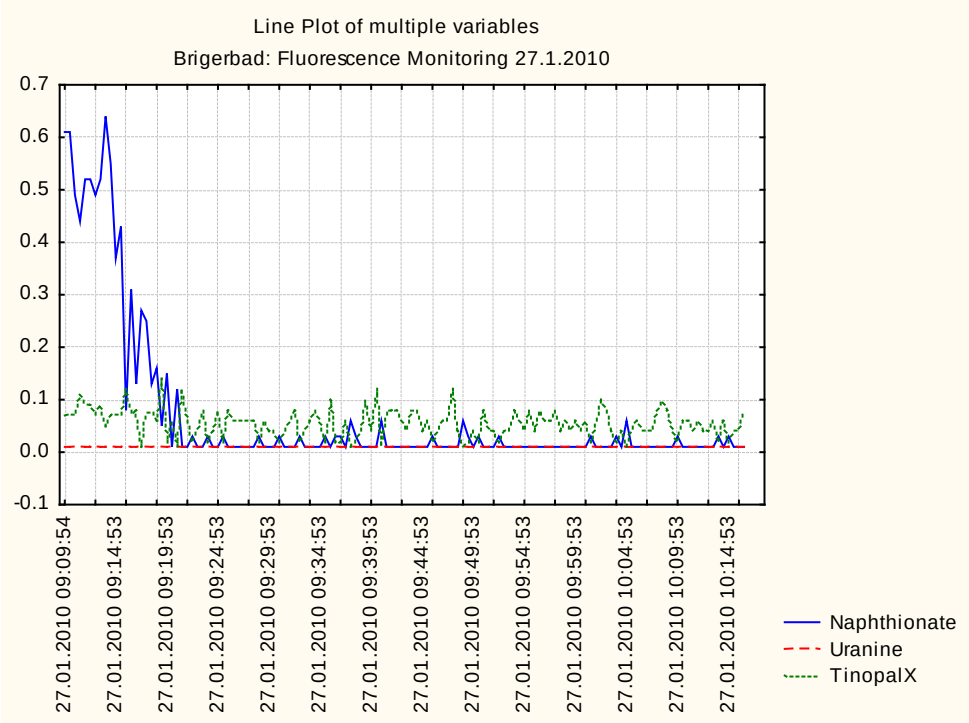

Fig. 16 Short monitoring period of 1 hour with Fluorometer installed at Brigerbad. The measurement of the specific wavelength domains of Tinipal X (green line), Naphthionate (blue line) and Uranine is represented.

4.3 Magnetotelluric measurements in Wallis area

Dr. Yassine Abdelfettah, Dr. Eva Schill, Centre d'hydrogéologie et de géothermie (CHYN), Université de Neuchâtel

The magnetotelluric (MT) is a passive geophysical prospection method. It belongs to the low frequency electromagnetic exploration methods. Its principle is based on the induction of the electromagnetic waves in the underground. The principal of the low frequency electromagnetic methods is the study of the fluctuations of the electromagnetic fields induced in the subsurface. Indeed, the induced electric currents (sometimes called telluric) circulate permanently in the underground. The associated electromagnetic fields are recorded on the surface of the earth. An adequate treatment on the measured electric and magnetic fields make possible to characterize the subsurface by its electrical conductivity.

The aim of this study is to identify a place, where long-term magnetic or magnetotelluric measurements can be carried out with the aim to observed changes in the electromagnetic field due to large earthquakes. Such changes have been observed and describe in different scientific studies. A review of such effects, which can be observed both in the electric and the magnetic field component in the frequency range of ULF (300Hz-3kHz) to VLF (3kHz-30kHz), is given in Johnston et al. (1997). Magnetotelluric measurements are often strongly influenced by anthropogenic noise. Thus, different sites were tested in particular for this artificial noise influence on the natural signal.

In this report, we will describe briefly the origin of the source, the fieldwork configuration, some theoretical aspect and MT Wallis data analysis. Further information about MT method are given in the following papers: Cagniard 1953, Vozoff 1991, Ward and Hohmann 1988, McNeice and Jones 2001, Baba et al. 2006 and therein references.

4.3.1 MT source

The electromagnetic fields recorded on earth surface are subdivided into two categories according to its origin; primary electromagnetic fields (or source) and secondary electromagnetic fields (or induction field). The origin of primary fields is external and for secondary fields is internal. The secondary electromagnetic fields are induced by the primary fields while diffusing in the conducting underground. The primary electromagnetic fields are generated mainly by the interaction of the sun wind with the terrestrial environment (Figure 17) for frequency lower than 1 Hz. For the higher frequencies (1-10 KHz), the source consists of atmospheric electric shocks (Vozoff 1986). To be noted that on the surface of earth, we record the superposition of these two kinds of electromagnetic fields and we can't extract the secondary field only.

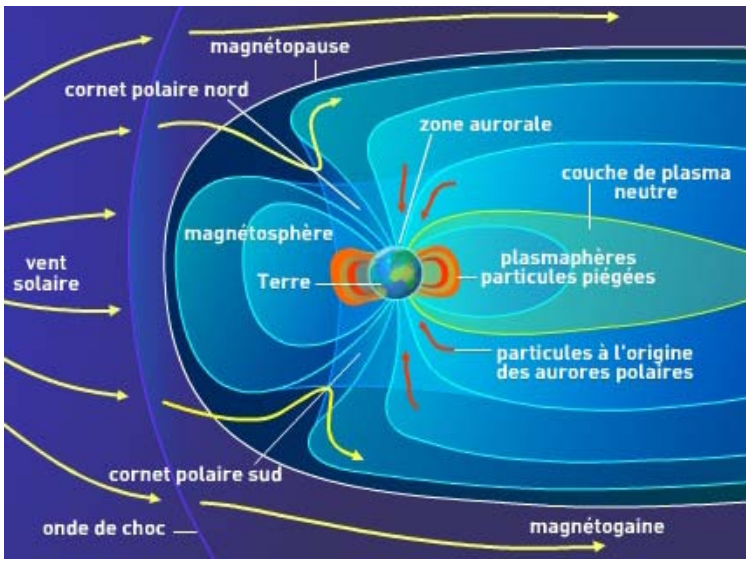

Fig. 17 The magnetotelluric source (So2media, 2009)

The advantage of the MT is that the source is free and is present almost at any time. The amplitude of the source signal is correlated directly with the solar activity. From that, it is important to know the prevision of the solar activity before doing MT measurement. For the Wallis MT measurement test, the solar activity was quiet (Figure 18). The MT measurement started from October 19 at 4.38 pm until October 21 at 5 am (see blue rectangle in Figure 18). This flat solar activity means that the energy of primary electromagnetic field is low. For the interpretation of the Figure 18 we take into account the Sub-Aurorale diagram which is valid for the zone situated under 55°N.

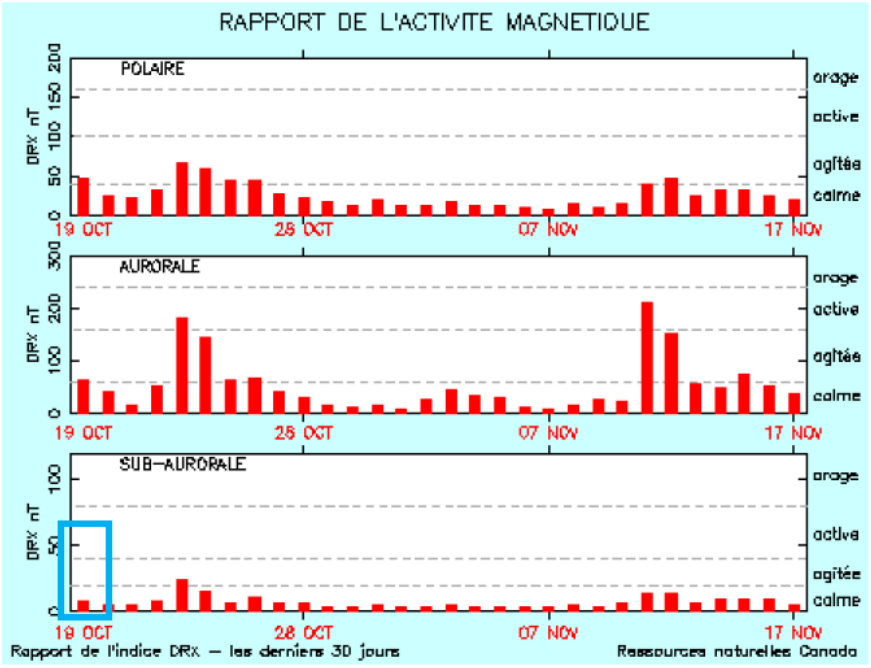

Fig. 18 Magnetic activity recorded between 19 October and 17 November 2010 (ISES, 2010)
Our test measurements are acquired between 19 to 21 Oct situated in blue rectangle.

4.3.2 Fieldwork

The acquisition of MT data requires the recording of two electromagnetic fields; electrical field and magnetic field. This recording is generally done continuously in the time domain. The recording of the electric field is done using four non polarizable electrodes in two perpendicular directions (Figure 10). The recording of magnetic induction is done using three magnetometers (or coils) recording three components of the magnetic field. We see in Figure 10 that ideally the area should have 100x100m to record the two components of electrical field and 5x5m to record the three components of magnetic field. Unfortunately, for our 3 MT sites, SIMPL, EMBD and VANNI, there is no possibility to record the electrical field.

4.3.3 From electromagnetic fields to subsurface characterization

In exploration campaign, we recorded 5 electromagnetic components: E_X, E_Y, H_X, H_Y and Hz, where E refers to the electrical field and H to the magnetic field. The relationship between E and H at any given frequency is described by the tensor Z as:

$$\begin{pmatrix} E_x(\omega) \\ E_y(\omega) \end{pmatrix} = \begin{pmatrix} Z_{xx}(\omega) & Z_{xy}(\omega) \\ Z_{yx}(\omega) & Z_{yy}(\omega) \end{pmatrix} \begin{pmatrix} H_x(\omega) \\ H_y(\omega) \end{pmatrix}$$

The components of Z are called also the MT transfer function. In the 1D area, the Z value can be expressed by

$$Z = \frac{E_x}{H_y} = -\frac{E_y}{H_x} = \sqrt{\frac{i\omega\mu}{\sigma}}$$

where σ is the electrical conductivity, it is the inverse of the electrical resistivity $\sigma=1/\rho$, $\omega=2\pi f$ is the angular frequency with f is a frequency and μ is the magnetic permeability for half space which is in general supposed equal to μ_0, magnetic permeability of free space. We remark in this formula that at any depth (or frequency), we can characterize the earth using only the ratio between electrical and magnetic fields if we know the electrical conductivity of the medium. Moreover, the vertical magnetic field H_Z is related to the horizontal fields H_X and H_Y by the Tipper complex vector T

$$H_Z = \begin{pmatrix} T_X & T_Y \end{pmatrix} \begin{pmatrix} H_X \\ H_Y \end{pmatrix}$$

Another important parameter for MT measurement is the skin depth δ, the depth at which de wave energy is attenuated by a factor $1/e$ (≈ 36.8%) to the surface magnitude. δ depends on a period $T=1/f$ used and on an electrical resistivity (Vozoff, 1991):

$$\delta = 0.5\sqrt{\rho\, T} \quad (km)$$

We remark that the vertical resolution for MT increase with increasing T and ρ and decrease with increasing σ and f. In Table 4, are some values for δ (km) with different f and ρ.

$\rho\ (\Omega.m)$ \ $f\ (Hz)$	500	1	0.01
1	0.02	0.5	5
10	0.07	1.5	15
1000	0.7	15	158

Table 4 Skin depth for isotropic media in km calculated for different frequency and electrical resistivity

4.3.4 MT data analysis in the Wallis

In the Wallis 4 MT tests were performed. We recorded continuously for 12h in the night and in three of the four sites (Vanni, Simpl, Embd), we recorded only the 3 components of magnetic field H_X, H_Y and Hz, since there is not enough space to record the 2 components of the electrical field (Figure 10). The frequency band covers 426–0.015 Hz. This frequency range overlaps with the ULF band, in which seismic precursors are expected to occur. The VLF band was not chosen, because conventional Metronix instruments cover only a part of it and a long-term record of this part leads to an enormous quantity of data. Thus, the amount of data would immediately fill the hard disk of the datalogger. The very strong anthropogenic signal is produced by the power lines with the dominant frequency of 50 Hz and its harmonics, as well as, the railways with a dominant frequency of 16 2/3 Hz in Switzerland.

The time series recorded with frequency sample of 2048 Hz at the four MT sites: Simpl, Embd, Vanni and Burchen, are shown in Figure 19. Using digital filter “mtx4x” or “mtx32x” (Friedrichs, 2008, Matzander, 2009), we recover the middle and the low frequency to increase the skin depth. In Figure 20, the time series for the same MT sites are shown with 4 Hz sample frequency. It should be noted that in the Burchen site, we recorded also and additionally to the magnetic field components the electrical components. This allows a complete data processing in order to obtain the variation of apparent resistivity and phase for the different frequencies.

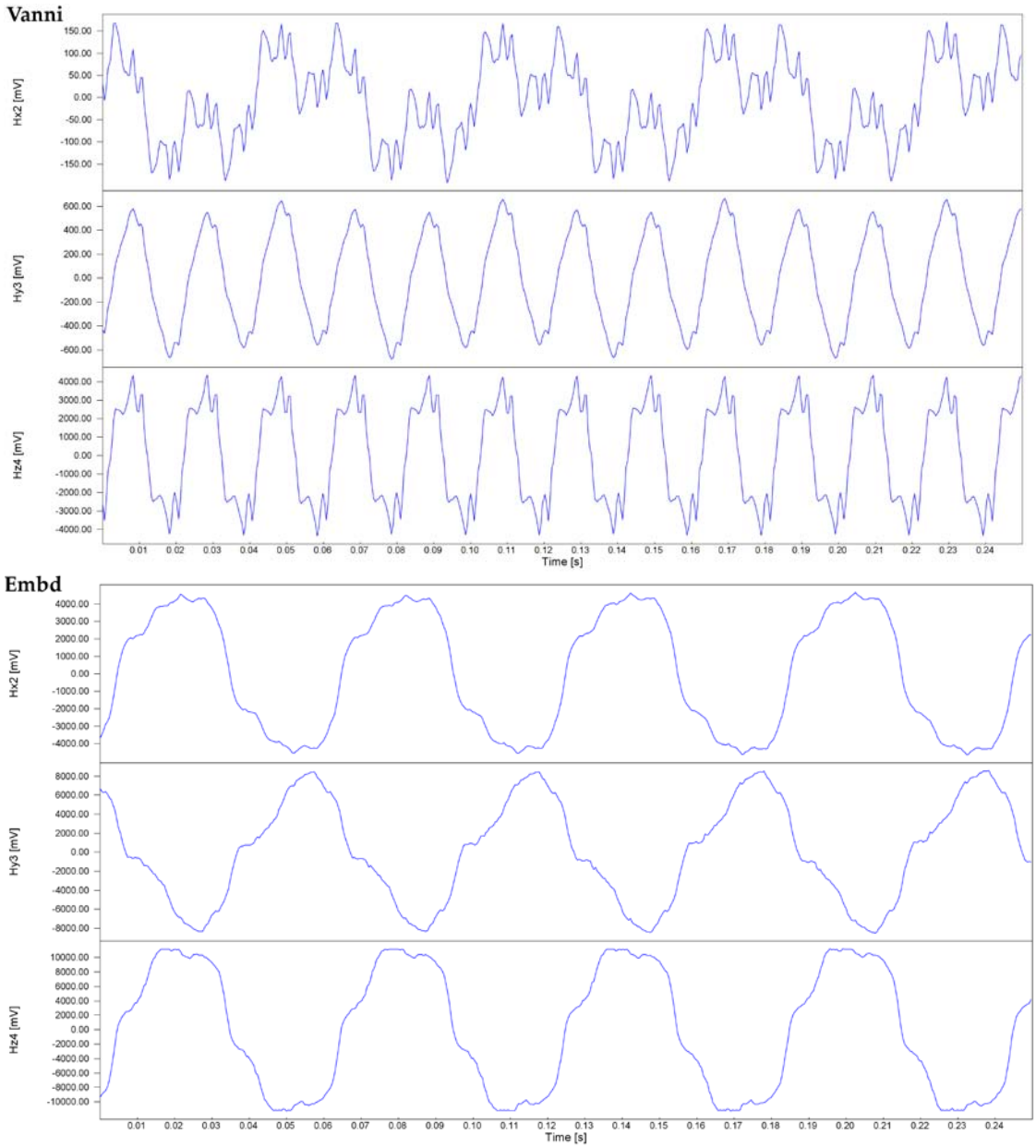
Vanni
Hx2 [mV]
Hy3 [mV]
Hz4 [mV]
Time [s]
Embd
Hx2 [mV]
Hy3 [mV]
Hz4 [mV]
Time [s]

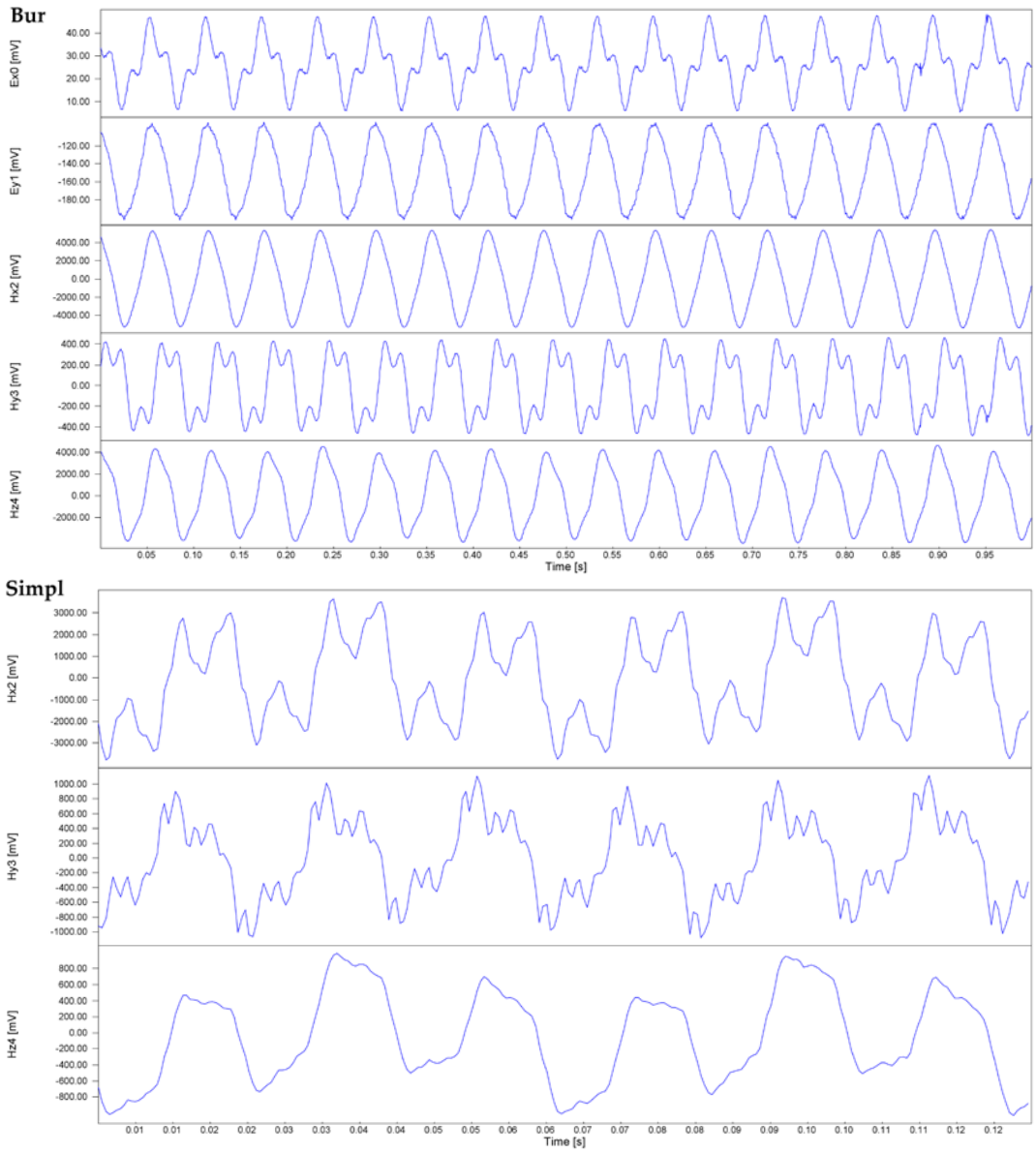

Fig. 19 Simpl, Embd, Vanni and Burchen MT Sites recorded with frequency sample of 2048 Hz and showed with different window length

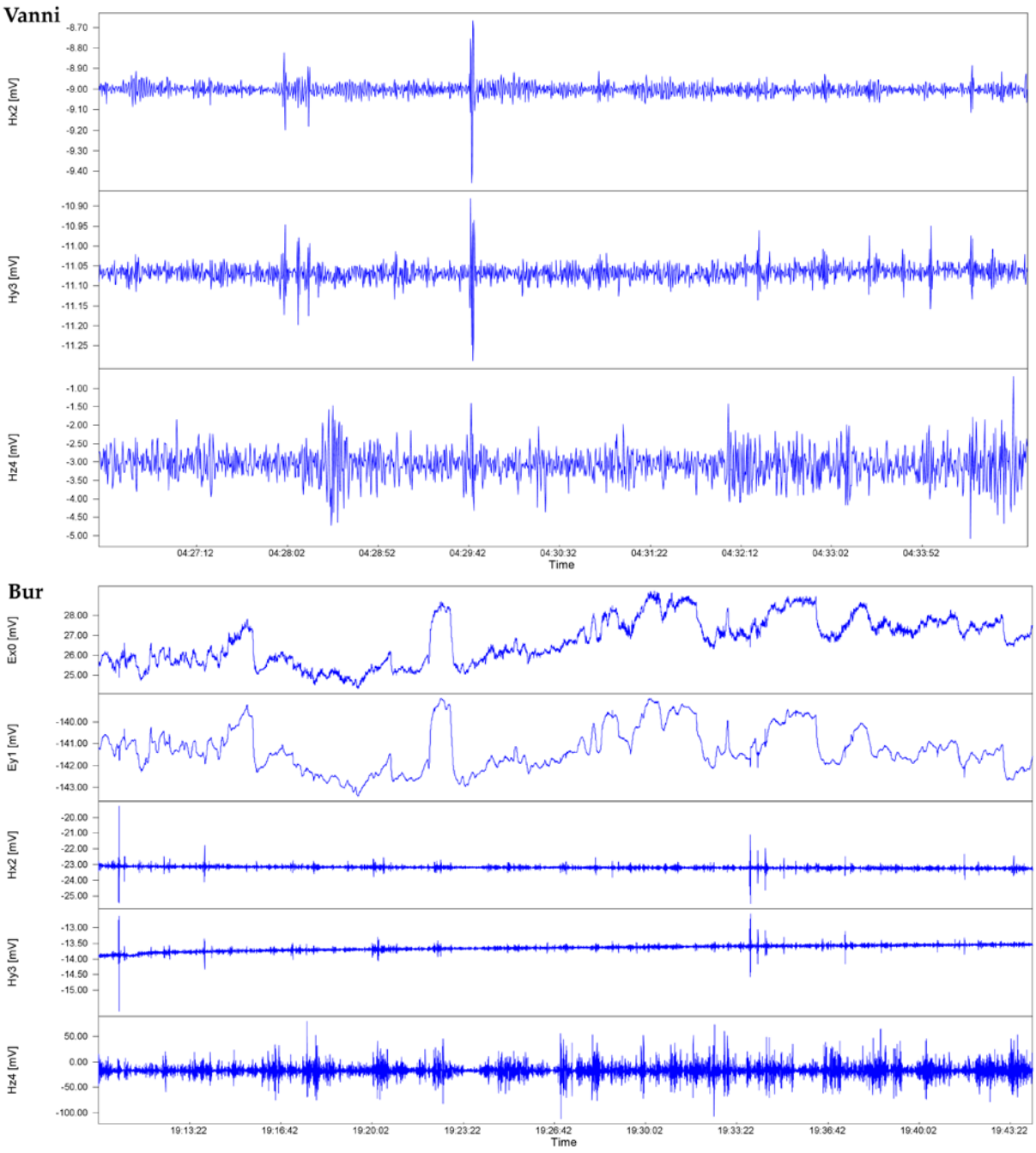
Vanni
Hx2 [mV]
-8.70
-8.80
-8.90
-9.00
-9.10
-9.20
-9.30
-9.40
Hy3 [mV]
-10.90
-10.95
-11.00
-11.05
-11.10
-11.15
-11.20
-11.25
Hz4 [mV]
-1.00
-1.50
-2.00
-2.50
-3.00
-3.50
-4.00
-4.50
-5.00
04:27:12
04:28:02
04:28:52
04:29:42
04:30:32
04:31:22
04:32:12
04:33:02
04:33:52
Time
Bur
Ex0 [mV]
28.00
27.00
26.00
25.00
Ey1 [mV]
-140.00
-141.00
-142.00
-143.00
Hx2 [mV]
-20.00
-21.00
-22.00
-23.00
-24.00
-25.00
Hy3 [mV]
-13.00
-13.50
-14.00
-14.50
-15.00
Hz4 [mV]
50.00
0.00
-50.00
-100.00
19:13:22
19:16:42
19:20:02
19:23:22
19:26:42
19:30:02
19:33:22
19:36:42
19:40:02
19:43:22
Time

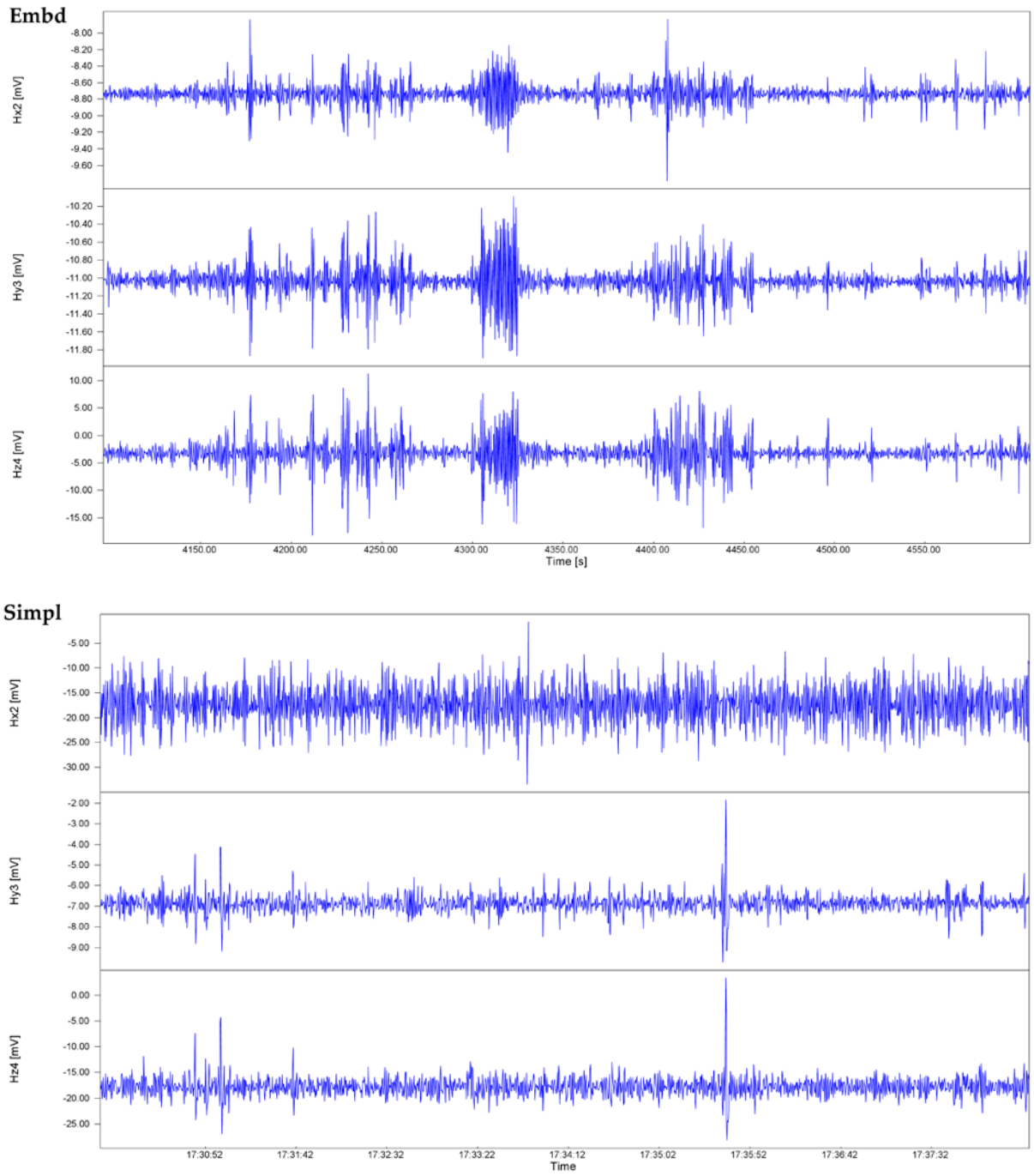

Fig. 20 Simpl, Embd, Vanni and Burchen MT Sites recorded with frequency sample of 4 Hz and showed with different window length.

To identify the different sources in the MT signal recorded and to have an idea about the artificial noise the spectral content has been analyzed. For example, in the spectral diagram of Embd site with sample frequency of 2048 Hz this noise (16 2/3 Hz and 50 Hz) can be clearly identified (Figure 21). Furthermore, in the higher frequencies the harmonics of both frequencies can be observed. To remove the power lines effect as well as the railways effect and its harmonics, we use a specific filter. It exists at least two ways to choose the adequate filter depending on the depth of target. For the Wallis MT data filtering, two approaches will be discussed.

1. Low pass filter: Using a low-pass filter allows cutting off the high frequencies. The low pass filter in general reduces the data by the number of a digital filter chosen. It means that if we choose a 32x digital filter, the times series will reduce by 32 times the input frequency. For example, to get a times series of 64 Hz, we filter the recorded times series recorded with 2048 Hz by 32x digital filter. Using the low pass digital filter, we lost the high frequencies. The times series recorded by sample frequency of 2048 Hz, it cover the frequency range between 425 and 12 Hz. If we filter this time series with 32x digital filter, we cover only the frequency range 12 to 0.9 Hz

   In this study, we used the digital filter incorporated in Mapros software (Metronix). In Figure 22, a sequence of spectra obtained after different digital filtering with frequencies: 512, 128, 32, 16 and 4 Hz is shown for Embd MT site. The spectrum content of H_x is representative for the artificial noise features for all 3 magnetic components. After filtering the 16 2/3 Hz and 50Hz artificial noise with a low pass filter the sample frequency is reduced to 16Hz. Thus the highest frequency obtained in the final time series is <4Hz. This shows that with this type of filter the ULF band cannot be assessed anymore. If we consider this frequency as the highest frequency, the shallow subsurface structures at a depth of less than 800 m (supposing 10 Ω.m mean resistivity of the subsurface) cannot be investigated.
2. Notch filter: This specific filter to cut the frequencies dominant in the artificial noise is incorporated in WinGLink software (Geosystems) to remove the 16 2/3 Hz and 50 Hz as well as its harmonics. This kind of filter allows removing specific constant values and we must specify all values as well as the harmonics values. The results of the Notch Filtering are showed in Fig. 23. We notice in this spectrum that the frequencies 16 2/3, 50 Hz and its harmonics 150, 250, 350, 450, 550, 650, 750, 850, 950 are removed.

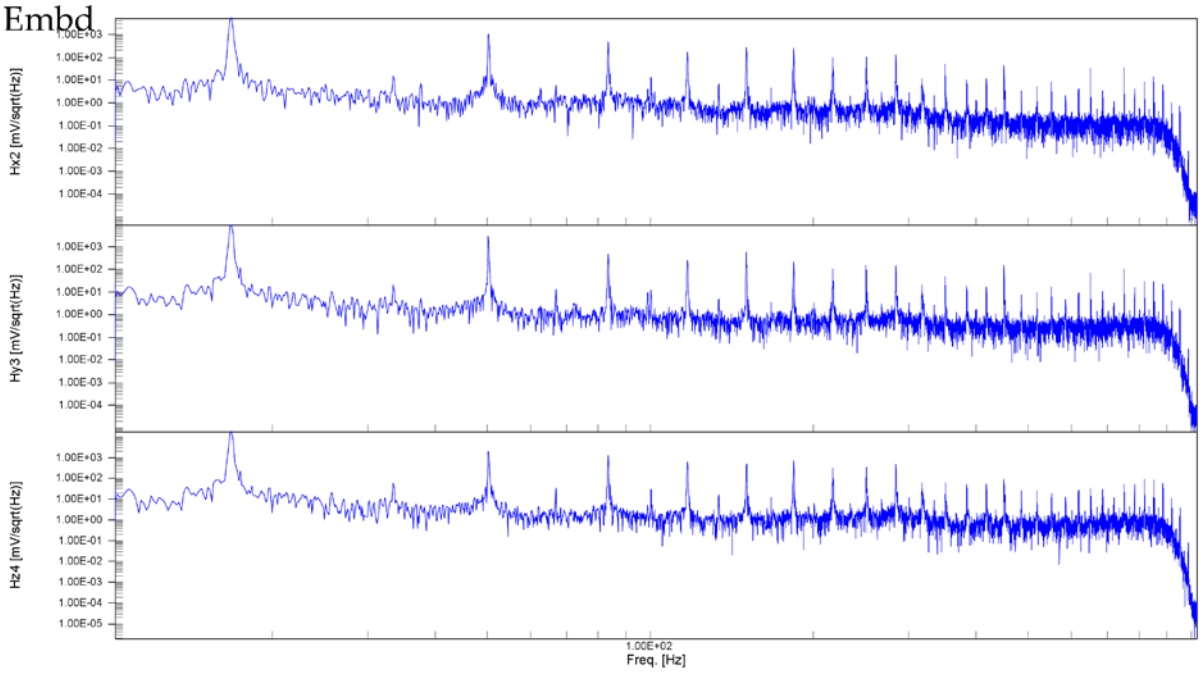

Fig. 21 Spectrum for times series recorded with 2048 Hz sample frequency for Embd MT site

An unexpected vagabond electrical current in the electrical field component is recorded in Burchen site, where the electric and magnetic components were registered (Figure 24). This effect is reflected in both the apparent resistivity and highly variable phase shift obtained for this site. At period greater

than 1s (or frequency less than 1Hz), the apparent resistivity increases up to 10^{11} Ω.m (Figure 25), which does not correspond to any resistivity known for the crust. The following explanation can explain this unusual behavior. The apparent resistivity ρ_{app} in the 1D case may computed by

$$\rho_{app} = 0.2T\left|\frac{E_x}{H_y}\right|^2$$

Thus, in order to obtain the same apparent resistivity at longer periods *T* increases, the ratio between Ex and Hy has to decrease. In the case of Burchen the apparent resistivity increases continuously with increasing period. This feature can be explained by the fact that the electrical component increases more quickly than the magnetic component in the greater periods. The behavior of the electrical and magnetic components can be seen in Figure 20. One possible explanation for the increases in the electrical field is the vagabond electrical current, which may be caused by the continuous current used in the some railways in the Wallis area.

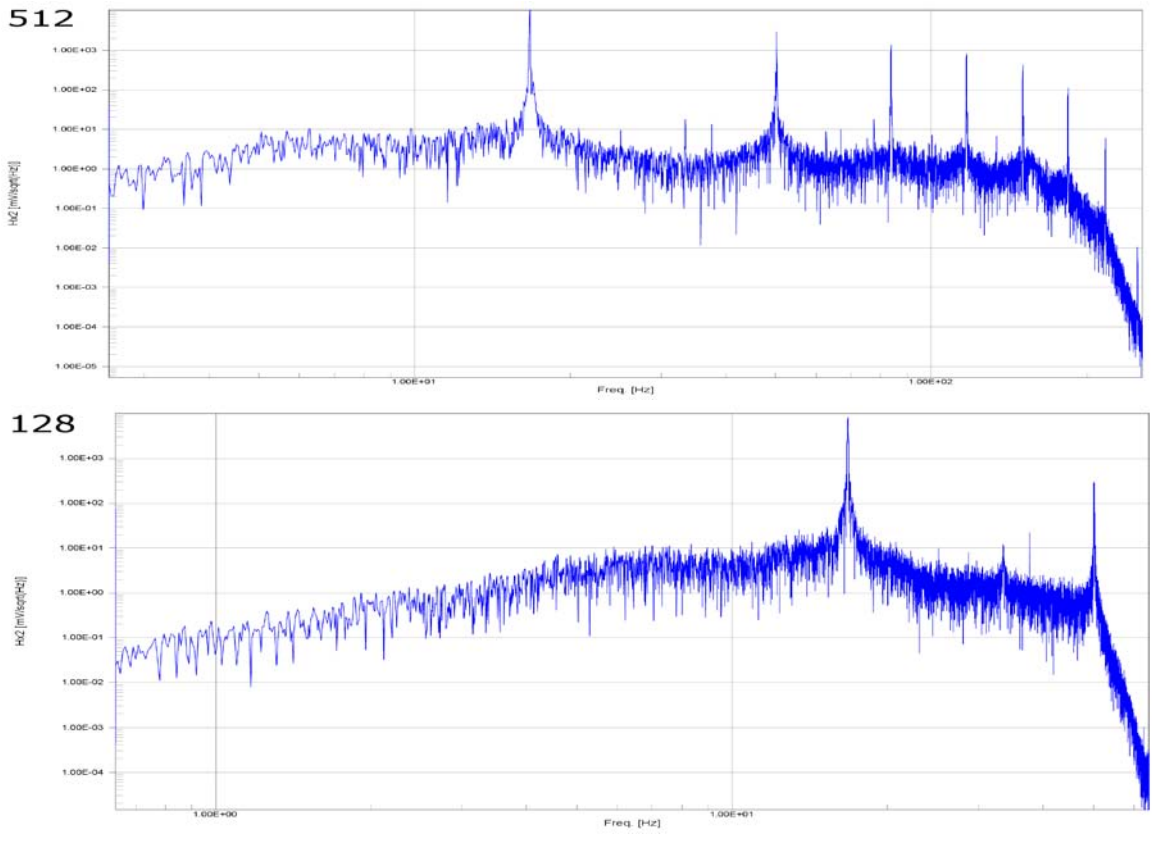

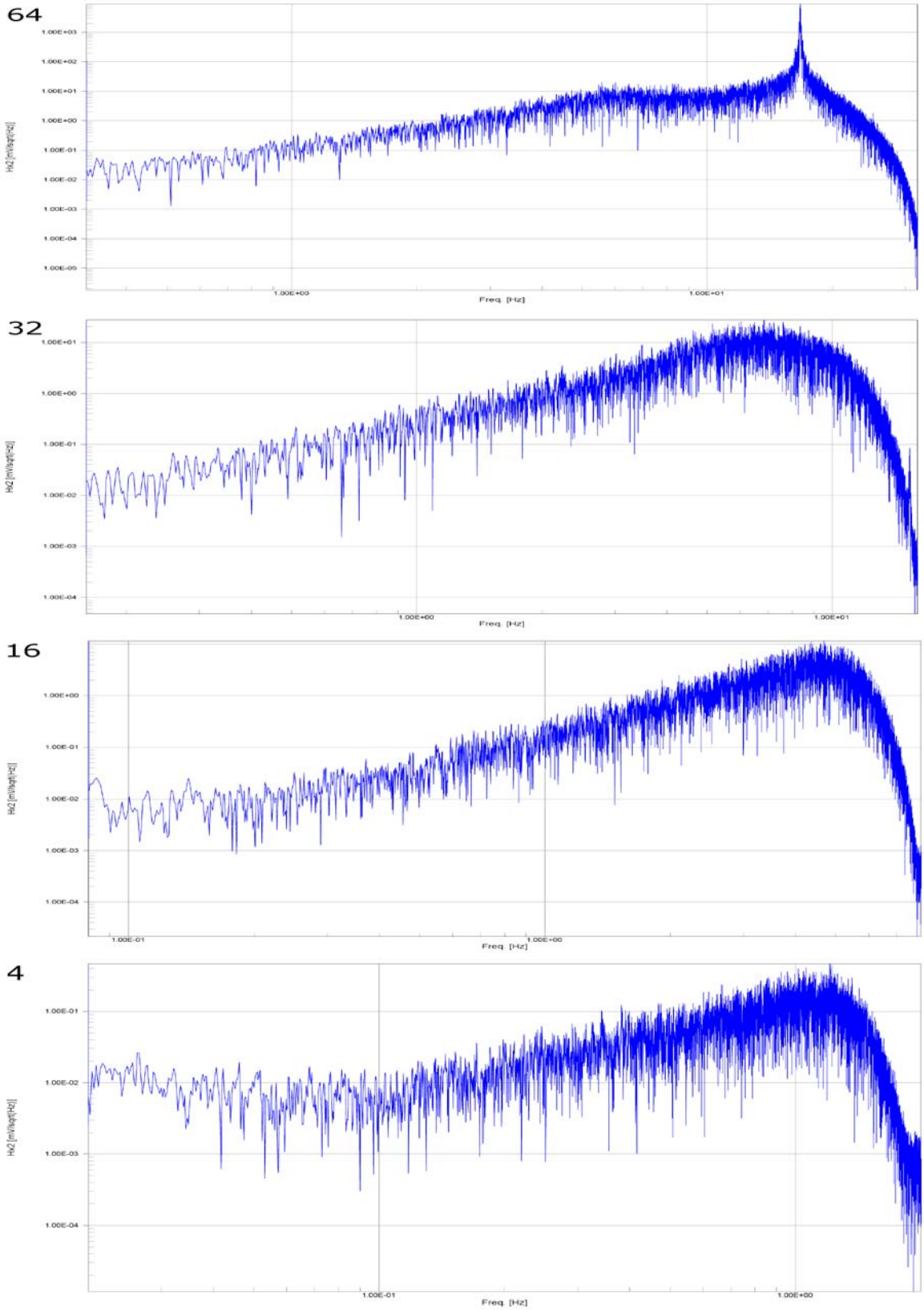

Fig. 22 A sequence of spectrum obtained after applied a specific low pass digital filter on time series recorded with sample frequency of 2048 Hz. The digital filters are 512, 128, 64, 32, 16 and 4 Hz for Embd site.

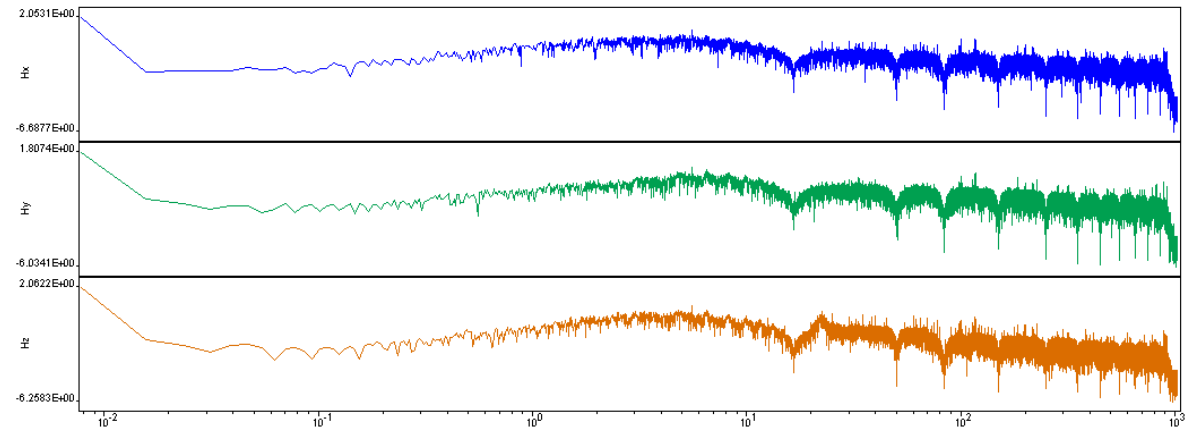

Fig. 23 Spectrum obtained after applied Notch filtering on time series recorded with sample frequency of 2048 Hz

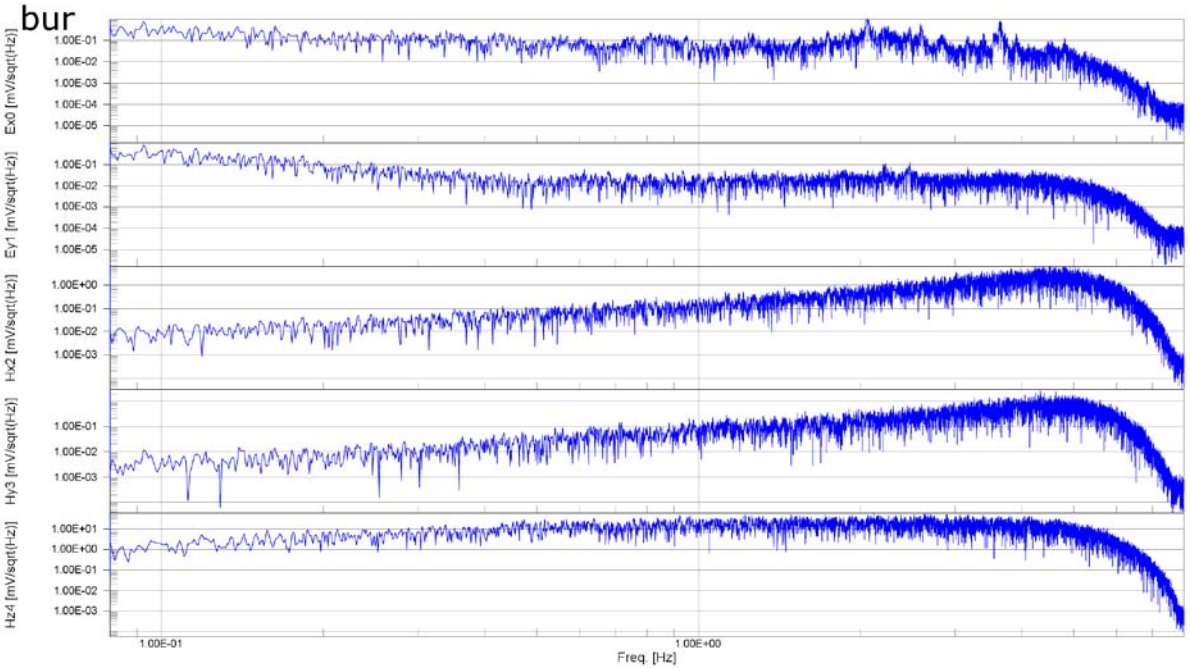

Fig. 24 Spectrum of E and H components obtained in Burchen site recorded with 16 Hz sample frequency. We note that with increasing the periods, the electrical component increase while the magnetic component decreases

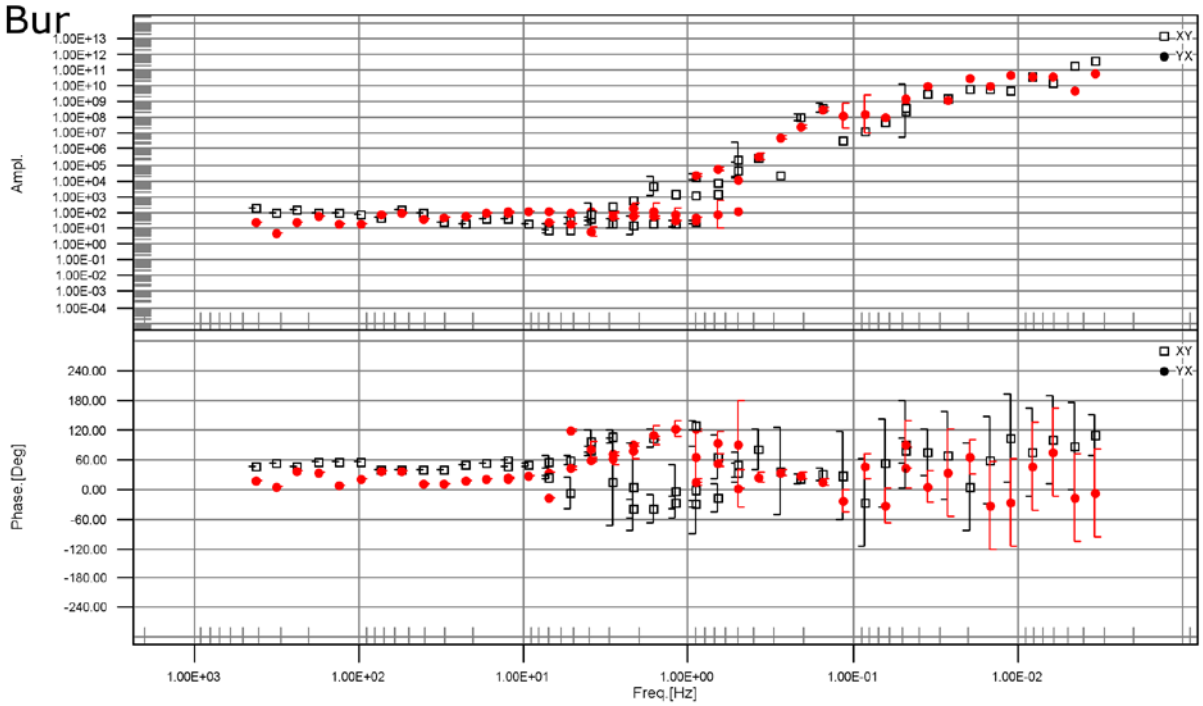

Fig. 25 Apparent resistivity and phase versus frequency for Burchen MT site

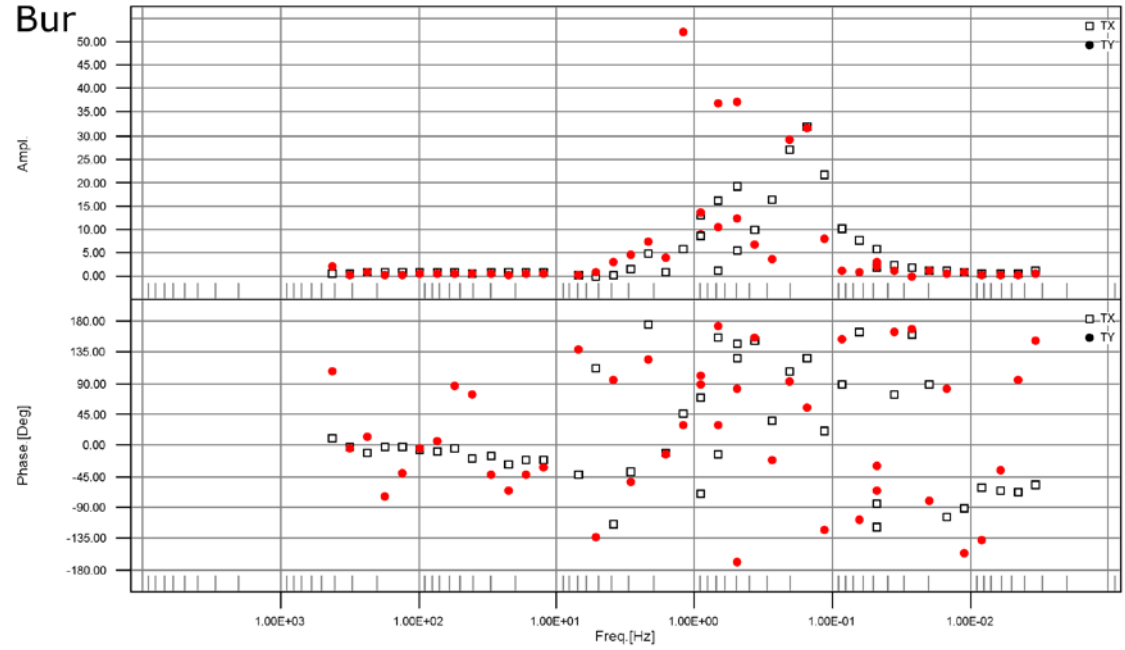

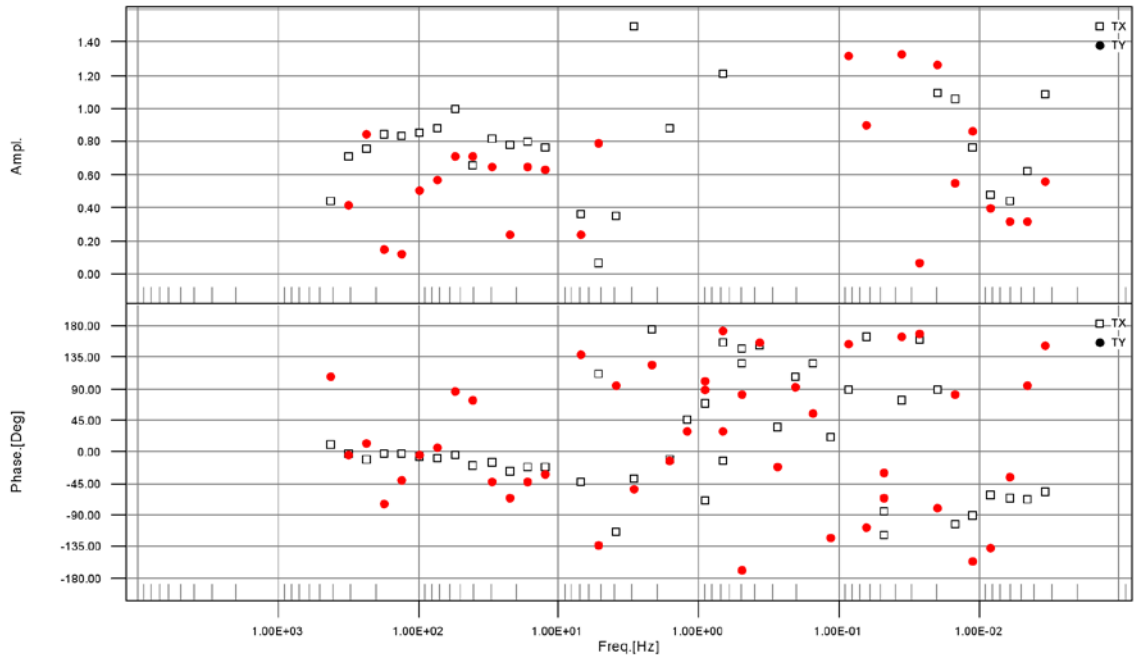

Fig. 26 Tipper amplitude and phase for Burchen MT site. Top) the high amplitude for Tipper components signified the high noisy signal. Usually, the tipper values are between 0 and 0.5 and rarely great than 1 (Vozoff, 1991). Here as we can observe the tipper values are greater than 50. These bad values were concentrated in the "dead band" where the magnetotelluric signal is weak in spite of the band here is large than the dead band; 0.02 to 5 Hz. It means that the recorded signal is dominated by the anthropogenic noise. It appears that the tipper is best in frequency range 425-5 Hz and <0.02 Hz but if we look with more accuracy (bottom) this "best" tipper values, it reveals also that these tipper values are bad because almost all of them are greater than 0.5

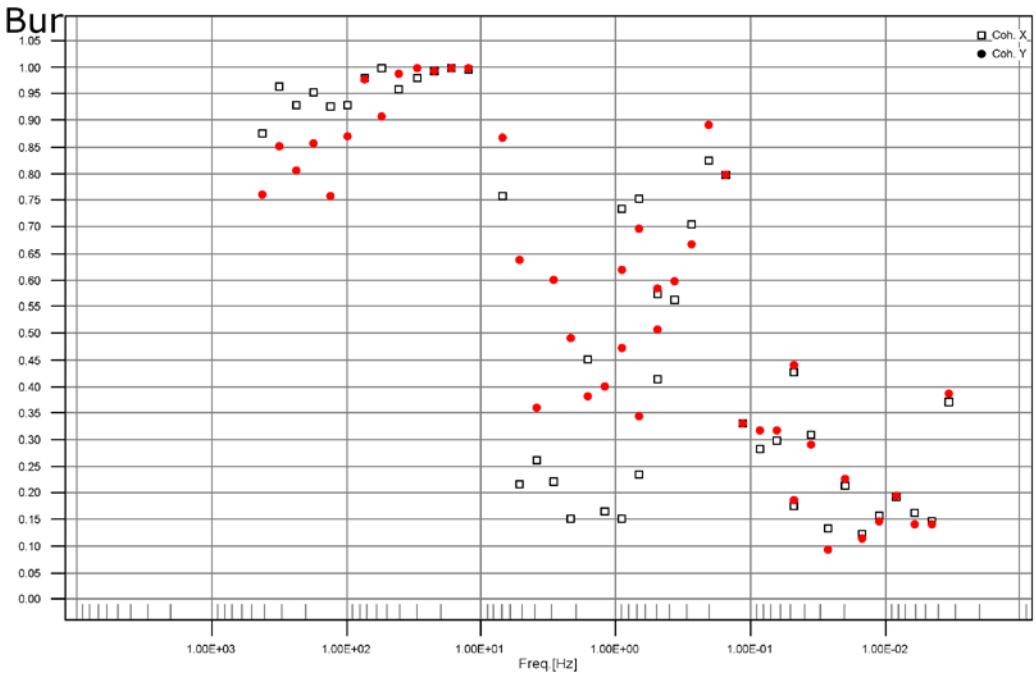

Fig. 27 The coherency between E and H components for Burchen MT site. The best result is obtained if the coherency is above 0.6–0.7 (Friedrichs, 2008). Note that the coherencies is bad for a frequency less than 5 Hz and the best coherency is reached for the frequencies greater than 5 Hz, especially between 10 and 100 Hz where the values are near the unity

4.3.5 Conclusions

Our study has shown that artificial noise is an important issue for magnetotelluric measurements in the Wallis. The 16 2/3 Hz and 50 Hz signals with their harmonics can be eliminated to a certain degree from the results. The vagabond currents at periods higher than 1s cannot be eliminated from the data. The frequencies of interest for the study of earthquake precursor however is in the range of >300Hz (e.g. Johnston, 1997).

From the point of view of the lowest anthropogenic noise the site Burchen, seem to be the most promising sites for setting up a permanent MT station in the Wallis with a general high noise level. It should be noted that the problem of vagabond currents in the Burchen site should be further investigated, since this type of noise cannot be filtered with conventional filters. However, these currents concern mainly the electric field, which due to weather conditions, in particular the intense thunderstorm activity in summer in Alps, is not recommended to acquire permanently.

Moreover, and in the case where only the magnetic fields components are recorded, tipper analyses (e.g. Figure 26) become necessary to evaluate the signal to noise (S/N) ratio and if desired to know more about the dimensionality of the medium (Vozoff, 1991). The tipper is sensitive to lateral changes in earth conductivity anomalies so it is useful to estimate the dimensionality of the subsurface. The magnitude of the tipper is zero for 1D case and between 0.1 to 0.5 for a major case and rarely great than 1. In the addition of this, the analysis of the H_zH_x and H_zH_y coherency supply the S/N ratio of the vertical magnetic field according to the both horizontal components. When the values are close to 1, the noise are neglected and when the values are close to 0.5 it means that the useful signal level is equal to noise level. It is important to record a minimum of three magnetic components during long time to access the S/N ratio. Likewise, it is possible to plot the coherency between E and H components (e.g. Figure 27).

For the continuation of the project, we recommend to investigate the existing literature on the phenomenon of changes in the magnetic field component due to natural seismic activity, in order to better define the frequency range at which an effect of seismicity is expected. In a second step, the possible electromagnetic tools should be re-evaluated, especially considering the possibility of data acquisition. It might be more suitable to install a permanent VLF station rather than a MT station.

5 First steps on non-seismic data streaming and dissemination

The non-seismic data discussed in the previous sections is planned to be transferred to the servers in SED and accessed by different solutions: COGEAR metadata frontend, GSN data stream and arclink server as discussed in Clinton et al., 2010 and Kästli and Fäh, 2011. In Figure 28, the data flow of the geochemical multi-sensor observations at Brigerbad is shown.

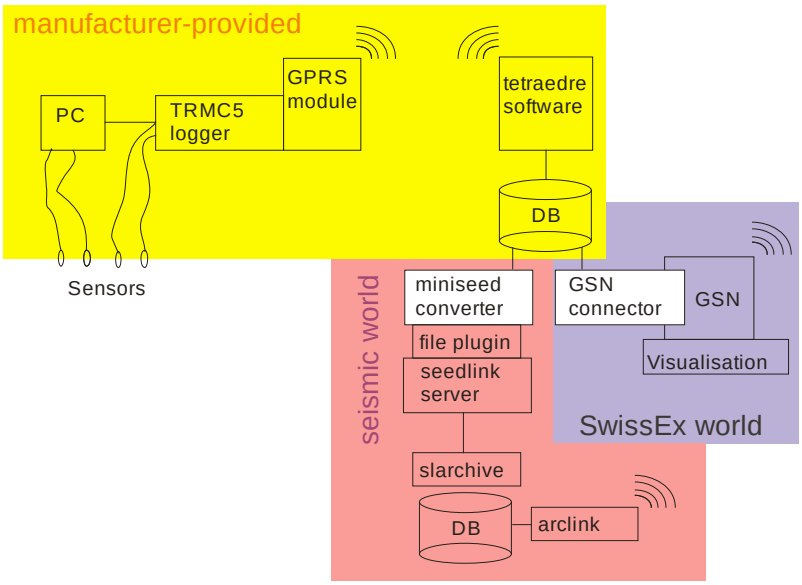

Fig. 28 Present end-to-end data architecture for real-time geochemical data (Kästli and Fäh, 2011)

At present a first phase of data retrieving is being implemented including the final data transmission to SED and storage scheme. The data recorded by the currently running geochemical systems, *M-54 Nucfilm* multi-sensor, *GGUN-FL30* field fluorometer, are hosted at the *Tetraedre* server and can be accessed via the internet http://multisensor.ethz.ch/manage (username and password are needed). The following scheme describes the steps to access the data:

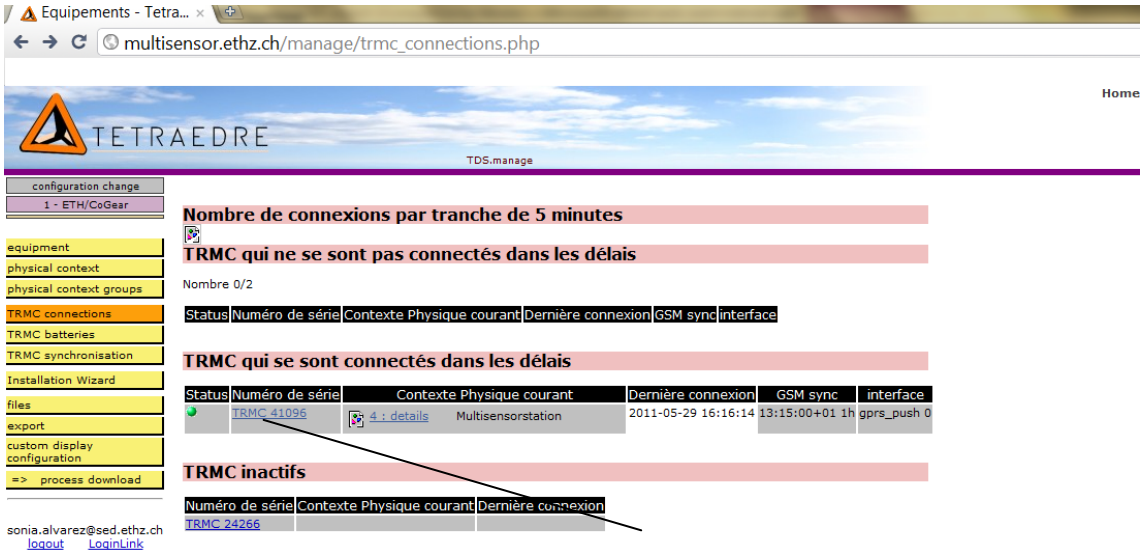

GGUN-FL30 fluorometer and *M_54* geochemical multi-sensor

Equipements du contexte

Edit	Fabricant	Modèle	Numéro de série
	Tetraedre	TRMC	41096

⇨ Modifier la liste des équipements

Mappings du contexte

Edit	Table input	Physical input	Measurement Set	a0	a1	a2	b0	c0	c1	c2
	acq_temperature	0	Multisensorstation, 1	0	3	255		1	1	1
	acq_albillia_fluo_delta	1	Multisensorstation, 1	0	0	255		1	1	1

⇨ Ajouter un mapping

Acquisitions et Mesures

⇨ Acquisitions (valeurs brutes)
⇨ Mesures (valeurs filtrées et traitées)

Link to fluorometer and geochemical multi-sensor data

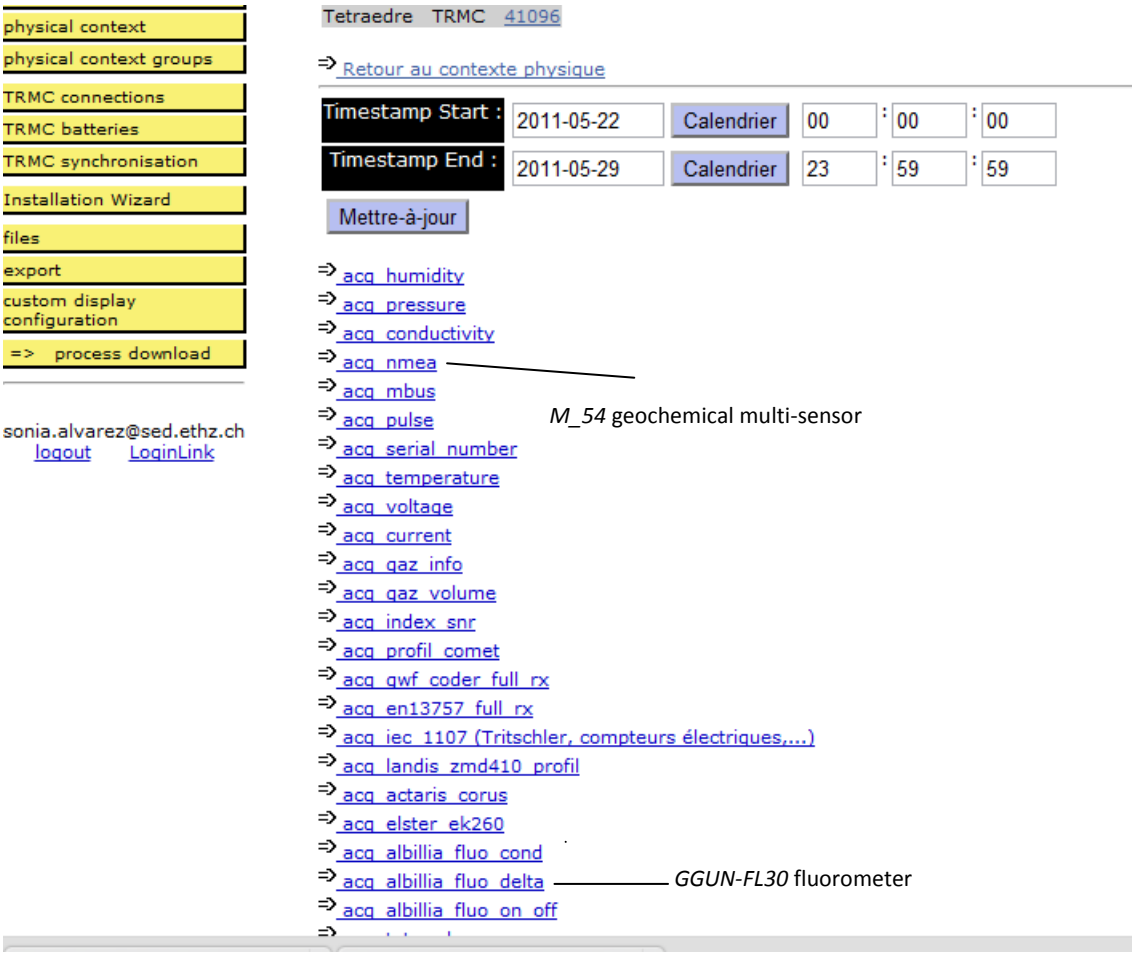

⇒ acq_albillia_fluo_on_off
⇒ acq_tetraedre

M 54 geochemical multi-sensor data

acq_nmea

temps_txt	physical_input	value	acquisition_id	timestamp	validated	converted	acq_index
2011-05-29 16:20:00	12.10.3.1	Y,2011,M,5,D,29,H,13,N,57,RN,3389,CO2,48,CH4,0,T1,290,T2,290,T3,340,Q,255,RH,258,VC,120	5294	1306678800	1	0	13
2011-05-29 15:20:00	12.10.3.1	Y,2011,M,5,D,29,H,12,N,57,RN,3431,CO2,48,CH4,0,T1,293,T2,293,T3,334,Q,254,RH,272,VC,120	5293	1306675200	1	0	13
2011-05-29 14:20:00	12.10.3.1	Y,2011,M,5,D,29,H,11,N,57,RN,3465,CO2,47,CH4,0,T1,282,T2,282,T3,334,Q,255,RH,262,VC,120	5292	1306671600	1	0	13
2011-05-29 13:20:00	12.10.3.1	Y,2011,M,5,D,29,H,10,N,57,RN,3338,CO2,47,CH4,0,T1,287,T2,285,T3,325,Q,254,RH,278,VC,120	5291	1306668000	1	0	13
2011-05-29 12:20:00	12.10.3.1	Y,2011,M,5,D,29,H,9,N,57,RN,3238,CO2,46,CH4,0,T1,261,T2,256,T3,308,Q,255,RH,245,VC,120	5290	1306664400	1	0	13
2011-05-29 11:20:00	12.10.3.1	Y,2011,M,5,D,29,H,8,N,57,RN,3305,CO2,45,CH4,0,T1,241,T2,235,T3,311,Q,259,RH,241,VC,119	5289	1306660800	1	0	13
2011-05-29 10:20:00	12.10.3.1	Y,2011,M,5,D,29,H,7,N,57,RN,3270,CO2,44,CH4,0,T1,261,T2,253,T3,299,Q,257,RH,258,VC,120	5288	1306657200	1	0	13
2011-05-29 09:20:00	12.10.3.1	Y,2011,M,5,D,29,H,6,N,57,RN,3333,CO2,43,CH4,0,T1,212,T2,212,T3,293,Q,257,RH,216,VC,120	5287	1306653600	1	0	13
2011-05-29 08:20:00	12.10.3.1	Y,2011,M,5,D,29,H,5,N,57,RN,3219,CO2,46,CH4,0,T1,215,T2,224,T3,322,Q,257,RH,204,VC,120	5286	1306650000	1	0	13
2011-05-29 07:20:00	12.10.3.1	Y,2011,M,5,D,29,H,4,N,57,RN,3317,CO2,47,CH4,0,T1,270,T2,267,T3,328,Q,255,RH,233,VC,120	5285	1306646400	1	0	13
2011-05-29	12.10.3.1	Y,2011,M,5,D,29,H,3,N,57,RN,3402,CO2,47,CH4,0,T1,270,T2,267,T3,328,Q,254,RH,233,VC,119	5284	1306642800	1	0	13

⇒ acq_actaris_corus
⇒ acq_elster_ek260
⇒ acq_albillia_fluo_cond
⇒ acq_albillia_fluo_delta
⇒ acq_albillia_fluo_on_off
⇒ acq_tetraedre

GGUN-FL30 fluorometer data

export Fluorimeter acquisitions as XML

acq_albillia_fluo_delta

temps_txt	physical_input	value	acquisition_id	timestamp	validated	converted	acq_index
2011-05-29 17:15:00	0	0.828207	253969	1306682100	1	0	4
2011-05-29 17:15:00	1	0.707954	253970	1306682100	1	1	5
2011-05-29 17:15:00	2	0.287294	253971	1306682100	1	0	6
2011-05-29 17:15:00	3	95.5379	253972	1306682100	1	0	7
2011-05-29 17:10:00	0	0.823736	253965	1306681800	1	0	4
2011-05-29 17:10:00	1	0.69946	253966	1306681800	1	1	5
2011-05-29 17:10:00	2	0.29996	253967	1306681800	1	0	6
2011-05-29 17:10:00	3	94.3607	253968	1306681800	1	0	7
2011-05-29 17:05:00	0	0.903755	253961	1306681500	1	0	4
2011-05-29 17:05:00	1	0.712424	253962	1306681500	1	1	5
2011-05-29 17:05:00	2	0.295938	253963	1306681500	1	0	6
2011-05-29 17:05:00	3	96.1241	253964	1306681500	1	0	7
2011-05-29 17:00:00	0	0.859052	253957	1306681200	1	0	4
2011-05-29 17:00:00	1	0.684858	253958	1306681200	1	1	5
2011-05-29 17:00:00	2	0.306069	253959	1306681200	1	0	6

6 References

Baba, K., Chave, A.D., Evans, R.L., Hirth, G. & Mackie, R.L., 2006. Mantle dynamics beneath the East Pacific Rise at 17°S: Insights from the Mantle Electromagnetic and Tomography (MELT) experiment, J. Geophys. Res., 111.

Bakun, W.H. & Lindh , A.G., 1985. The Parkfield, California, Earthquake Prediction Experiment, Science, 229, 619-624.

Balderer W, Leuenberger F, et al. (2002). Effects of the Cinarcik - Ismit August 17, 1999 earthquake on the composition of thermal and mineral waters as revealed by chemical and isotope investigations. Geofísica Internacional 41(4): 385-391.

Bernardi, A., A. C. Fraser-Smith, P. R. McGill, and O. G. Villard (1991), ULF magnetic field measurements near the epicenter of the Ms 7.1 Loma Prieta earthquake, Physics of the Earth and Planetary Interiors, 68(1-2), 45-63.

Bleier, T. and F. Freund (2005). "Earthquake alarm." IEEE Spectrum 42(12): 16-21 (int).

Cagniard, L., 1953. Basic theory of the magneto-telluric method of geophysical prospecting, Geophysics, 18, 605-635.

Cicerone, R.D.E., John E. & Britton, J., 2009. A systematic compilation of earthquake precursors, Tectonophysics, 476, 371-396.Lomnitz, C. (1994). Fundamentals of Earthquake Prediction. New York, John Wiley & Sons.

Clinton J., Kästli P., Fäh D. (2010). Seismic instrumentation in the Valais. Project Swiss Experiment. Deliverable for WP 4.6. Swiss Seismological Service ETH Zürich.Report SED/SwissEX/R/001/20101010.

Flynn R.,Hacini Y.,Schnegg P.-A.,Costa R.,Diomande.(2006) : Use of tracer tests and geophysical logging to understand solute and micro-organism tracer responses in monitoring wells with long screen intervals in a gravel aquifer; Beiträge zur Hydrogeologie, 55, 5-20.

Friedrichs Bernhard, 2008. MAPROS. http://88.198.212.158/mtxweb/uploads/media/mapros.pdf, pp. 1–123.

Fraser-Smith, A.C., Bernardi, A., McGill, P.R., Ladd, M.E., Helliwell, R.A. & Villard Jr, O.G., 1990. Low-frequency magnetic field measurements near the epicenter of the Ms 7.1 Loma Prieta Earthquake, Geophysical Research Letters, 17, 1465-1468.

Geiermann J, Schill E. (2010) 2-D Magnetotellurics at the geothermal site at Soultz-sous-Forêts: Resistivity distribution to about 3000 m depth. Comptes Rendus Geoscience 342 (7-8):587-599. doi:DOI: 10.1016/j.crte.2010.04.001

Geller, R. J. (1991). "Shake-up for earthquake prediction." Nature 352(6333): 275-276.

Hayakawa, M., Kawate, R., Molchanov, O.A. & Yumoto, K., 1996. Results of ultra-low-frequency magnetic field measurements during the Guam Earthquake of 8 August 1993, Geophys. Res. Lett., 23, 241-244.

Hayakawa M, Kopytenko Y, Smirnova N, Troyan V, Peterson T (2000) Monitoring ULF magnetic disturbances and schemes for recognizing earthquake precursors. Physics and Chemistry of the Earth, Part A: Solid Earth and Geodesy 25 (3):263-269.

Hayakawa, M., Hattori, K. & Ohta, K., (2007). Monitoring of ULF (Ultra-Low-Frequency) Geomagnetic Variations Associated with Earthquakes, Sensors, 7, 1108-1122.

Igarashi, G., S. Saeki, et al. (1995). "Ground-Water Radon Anomaly Before the Kobe Earthquake in Japan." Science 269 (5220): 60-61.

ISES, 2010. Centre régional d'avertissement pour le Canada. www.spaceweather.gc.ca. Consulted November 18.

Johnston, M.J.S., 1997. Review of Electric and Magnetic Fields Accompanying Seismic and Volcanic Activity, Surveys in Geophysics, 18, 441-476.

Kästli, P & Fäh, D. 2011. Instrumentation in COGEAR: SwissEx Progress-ETH CCES Projekt 2008-2012

Workshop 11.07.2011, ETHZ. Powerpoint presentation.

Kopytenko, Y.A., Matiashvili, T.G., Voronov, P.M., Kopytenko, E.A. & Molchanov, O.A., 1993. Detection of ultra-low-frequency emissions connected with the Spitak earthquake and its aftershock activity, based on geomagnetic pulsations data at Dusheti and Vardzia observatories, Physics of the Earth and Planetary Interiors, 77, 85-95.

Matzander, U. & Willms, M., 2009. ADU-07 operating Manual, Metronix Measurments and Electronics ltd, pp. 1–142.

McNeice, G.W. & Jones, A.G., 2001. Multisite, multifrequency tensor decomposition of magnetotelluric data, Geophysics, 66, 158-173.

Molchanov, O.A., Kopytenko, Y.A., Voronov, P.M., Kopytenko, E.A., Matiashvili, T.G., Fraser, Smith, A.C. & Bernardi, A., 1992. Results of ULF magnetic field measurements near the epicenters of the Spitak (Ms = 6.9) and Loma Prieta (Ms = 7.1) earthquakes: Comparative analysis, Geophys. Res. Lett., 19, 1495-1498.

Montgomery, D. R. and M. Manga (2003). Streamflow and Water Well Responses to Earthquakes. Science 300(5628): 2047-2049.

Nagao, T., et al. (2002), Electromagnetic anomalies associated with 1995 Kobe earthquake, Journal of Geodynamics, 33(4-5), 401-411.

Park, S. K., M. J. S. Johnston, T. R. Madden, F. D. Morgan, and H. F. Morrison (1993), Electromagnetic precursors to earthquakes in the Ulf band: A review of observations and mechanisms, Rev. Geophys., 31(2), 117-132.

Pulinets S, Boyarchuk K (2004) Ionospheric Precursors of Earthquakes. Springer

Schnegg P-A (1998) The magnetotelluric survey of the penninic Alps of Valais. Matériaux pour la Géologie de la Suisse Géophysique (32)

Schnegg P.A.(2003) : A new field fluorometer for multi-tracer tests & turbidity measurement applied to hydrogeological problems.; Proc. Of the 8th International Congress of the Brazilian Geophysical Society & 5th Latin American Geophysical Conference, Rio de Janeiro, Brazil.

Surbeck, H., Deflorin, O., Kloos, O. (2006), Spatial and temporal variations in the uranium series background in Alpine groundwaters, In : Uranium in the Environment, Mining Impact and Consequences, B.J.Merkel & A.Hasche-Berger (Eds.), Springer-Verlag, Berlin, Heidelberg, p.831-839.

Roeloffs, E., E. Quilty, and C. H. Scholtz (1997), Case 21 water level and strain changes preceding and following the August 4, 1985 Kettleman Hills, California, earthquake, Pure and Applied Geophysics, 149(1), 21-60.

Segvi, L. (2007). "A critical review on electromagnetic precursors and earthquake prediction." Turk J Elec Engin 15(1): 1-15.

So2media, 2009. La magnétosphère terrestre pour la csi. La cité des sciences et de l'industrie www.cite-sciences.fr, Consulted January, 23.

Süer, S., N. Güleç, et al. (2008). Geochemical Monitoring of Geothermal Waters (2002–2004) along the North Anatolian Fault Zone, Turkey: Spatial and Temporal Variations and Relationship to Seismic Activity. Pure and Applied Geophysics 165(1): 17-43.

Thomas, D., 1988. Geochemical precursors to seismic activity, Pure and Applied Geophysics, 126, 241-266.

Thomas, J. N., J. J. Love, and M. J. S. Johnston (2009), On the reported magnetic precursor of the 1989 Loma Prieta earthquake, Physics of the Earth and Planetary Interiors, 173(3-4), 207-215.

Vozoff, K., (1986). Magnetotelluric methods. Society of Exploration Geophysicists, 1–763.

Vozoff K (1991) The magnetotelluric method, in Electromagnetic methods in applied geophysics. M.N. Nabighian, vol 2, part B. Society of Exploration Geophysicists, Tulsa, Oklahoma, 641-711.

Wakita, H., Y. Nakamura, et al. (1988). "Short-term and intermediate-term geochemical precursors." Pure and Applied Geophysics 126(2), 267-278.

Wakita, H., Y. Nakamura, et al. (1991). Short-term and intermediate-term geochemical precursors. In evaluation of proposed earthquake precursors (Ed. M. Wyss). AGU, Washington, DC.

Wakita, H. (1996). Geochemical challenge to earthquake prediction. *Earthquake prediction: the scientific challenge*. National Academy of Sciences in Irvine, CA, Proc. Natl. Acad. SCI. USA. **93:** 3781-3786.

Walia, V., H. S. Virk, et al. (2006). Radon Precursory Signals for Some Earthquakes of Magnitude > 5 Occurred in N-W Himalaya: An Overview. Pure and Applied Geophysics 163(4): 711-721.

Wang K, Chen Q-F, Sun S, Wang A (2006) Predicting the 1975 Haicheng Earthquake. Bulletin of the seismological society of America (3):757-795.

Ward, S. H. and G. W. Hohmann, 1988. Electromagnetic theory for geophysical applications. In. Applied Geophysics. Ed. M.N. Nabighian, 1, pp. 131–311

Wyss, M. (1991). "Evaluation of proposed earthquake precursors (ed. M. Wyss)." AGU, Washington,DC: 94.

Wyss, M. and D. C. Booth (1997). "The IASPEI procedure for the evaluation of earthquake precursors." Geophysical Journal International 131(3): 423-424.

Wyss, M. (1997). "Second round of evaluations of proposed earthquake precursors." Pure and Applied Geophysics 149(1): 3-16.

Wyss, M. (2001). Why is earthquake prediction research not progressing faster?. Tectonophysics 338(3-4): 217-223.

Woith, H., R. Wang, et al. (2003). Heterogeneous response of hydrogeological systems to the Izmit and Düzce (Turkey) earthquakes of 1999. Hydrogeology Journal 11(1): 113-121.

Appendix: Actions taken during the installation of the first geochemical multi-sensor system in Brigerbad

Event (date, information)	Reported by	Date of report	Comments
On the sensors to be installed in Brigerbad	Heinz Surbeck	2010.02.20	Other sensors could be added. However I don't recommend to measure pH continuously. It is unreliable unless recalibrated very frequently.The fluorimeter used at Brigerbad already has a temperature measurement. I'll ask if it also has a conductivity probe, or if it would be available as an option. If not, I could ad one as an option to my offer. There are reasons that I did not offer it. Conductivity probes have to be cleaned frequently at highly mineralized springs. In addition spring water frequently is gas-oversaturaded leading to bubble formation on the electrodes. This gives erratic readings. To my experience radon, CO2 and other gases like methane react far stronger to changes in the acquifer than other parameters like temperature, conductivity or pH. Helium also seems to be a good indicator for changes deep down, but to measure it continuously in the field is not so easy
Sending fluorometer to test	Werner Balderer (sent to P.-A. Schnegg)	2010.08.18	J'ai une question concernant notre Fluorometre installé à Brigerbad pour mesurer la fluoresence naturelle: Il semble en comparaison avec les mesures sur échantillons journalières par spectromètre au labo que la sensivité du fluorometre s'est diminué. Est-ce que nous pourrions vous envoyer le fluorimetre pour test et revision. Une question est aussi si vous avec maintenant des diodes plus puissantes ou plus spécifiques pour la domaine qui nous interesse entre 310-355 et 370 – 410 nm.
2011.11.05 1st installation of the fluorometer	Werner Balderer (sent to R. Tanner)	2010.11.09	ich habe den Fluorometer letzten Freitag installiert, na Test in unserem Labor. Der Test war einwandfrei, doch bin ich nach der Installation nicht ganz sicher ob der Kanal von Tracer 3 auch funktioniert. Wann gehst Du wieder ins Wallis? Eventuell würde ich wieder mitkommen.

2011.01.26, 14.30; 2011.01.28, 16.00 2nd installation of the fluorometer. Adjustments	Werner Balderer (sent to P.-A. Schnegg)	2011.02.01	J'ai installé le fluorometre le 26 Janvier à 14.30 à Brigerbad à 16h et le 28 j'ai changé juste la position du fluorometre dans le bassin de la source de environ 30 cm. Je me demande maintenant que le LED 2 et 3 ont arrêté de fonctionner après environ 1 jour et je vous envoie les fichier correspondant enregistré par tétraèdre.
Replacement of the fluorometer	Werner Balderer	2011.02.02	I have last Friday replaced the fluorometer together with George Arnold from Brigerbad. He indicated me the place according to him with higher temperature, where he collects also the sample for us for fluorescence spectroscopy and chemical analyses every day. But also there the water is only at a temperature of 37 °C. The temperature is for us not so important as the fact that sample properties and on-line measurements are comparable. So this site will remain fixed, but according to the resulting low level of the measurement signals, we will decide to try another modification of the fluorometer.
2011.04.19 Installation date of the geochemical multi-sensor	Heinz Surbeck	2011.04.21	The Rn/CO2/CH4 monitor has been installed this Tuesday (19.04.2011) and is working properly. I've checked it today. The water flow rate through the instrument is actually very low to avoid condensation in the sensors. During the next two weeks I will increase the water flow rate in several steps. After each step I have to check that the humidity in the measuring circuit is not going above 90 %. After that tuning the temporal resolution should be on the order of 1 h.
First tunings of the Monitor	Heinz Surbeck	2011.05.02	I've now been several times at Brigerbad to tune the Monitor. The water flow is now at it's nominal value of 1500 ml/h. This means that it takes 30 min for the water to be pumped from the spring to the monitor. The radon concentration is so high (50 Bq/l) that I had to reduce the counting time to avoid counter overflow. According to Georges Arnold from the Brigerbad they are more or less pumping constantly from TQB1. This results in a temperature at the spring of around 32 to 34 C. This corresponds well to the temperature measured by Werner's instrument. Without pumping the water temperature can reach 50 C. Pumping will go on until November 1 when they close the spa for this year.

2011.05.19, 10:00 UTC Replacement of the water pump	Heinz Surbeck	2011.05.21	May 19, around 10:00 UTC I've replaced the water pump by a stronger one. The higher flow rate leads to a higher radon concentration in the measuring gas circuit. (see Figure 29). The CO2 concentation is less dependent on the water flow rate as diffusion through the exchange tube is far faster for CO2 than for radon.
2011 05 23 10:00 UTC Water pumps tested, variation water flow rate	Heinz Surbeck	2011.05.23	Today 23 May around 10:00 UTC I've tested different water pumps and have varied water flow rate several times. So don't worry if you notice sudden changes in the transmitted data. Seems that I've found an optimum for the flow rate. The water pump now installed is a high quality pump, said to have a long lifetime, especially as it runs only during 20% of the time. I'll now follow the development of the data. If everything looks good during the next weeks I will consider installation to be completed.
2011.06.06 late afternoon/2011.06.09 Problems with water tube	Heinz Surbeck	2011.06.10	Monday June 6 late afternoon data from the monitor have shown that there was no longer fresh water arriving from the spring. Therefore radon and CO2 values have dropped dramatically. Today, June 9 I've checked the water pump and the tube from the spring to the monitor. The pump is o.k., but the tube showed to be squezzed at two places. I've fixed it and now it's working again. I've also increased the water flow rate once again to about 2500 ml/h. This will result in a faster reaction to changes in the water composition at the spring. At the spring I've noticed that there is quite a lot of sludge or algea on top of the fluorescence monitor. Think it needs regular cleaning.
2011.06.17 17h UTC Drop CO2 2011 06 20 pump replacement	Heinz Surbeck	2011.06.20	June 17 around 17h UTC a sharp drop in CO2 and Rn values has shown that there is once again no fresh water arriving at the monitor. I've checked tubes and the water pump today June 20. The water pump has failed, probably because of a clogging of the valves by mud from the spring (iron hydroxides or algea). I've replaced the pump by one that seems to be less influenced by mud but has a lower flow rate. Actual flow rate is thus back to about 1500 ml/h. The pump will be sent back to factory to find out what may be the reason for the failure.
Different changes in the	Werner Balderer	2011.06.23	Here the latest exchange and instrument modifications of the Engineering Geology's fluorometer. With Mr. Schnegg à Neuchâtel. For the further track here the latest changes at Brigerbad: I have given the instrument for a last modification (removal of the filters at

fluorometer			the emission side: filtres Wratten 2A des trois optiques de détection) on the 21 February 2011 and got it back modified on the 28. February 2011. Then I have reinstalled the instrument on the 16. March 2011. The instrument was later removed by Robert Tanner and replaced by the Geophysics own instrument and datalogger / on-line transmission system on the 20 April 2011 (see mail). The BIBAG instrument is identical with our fluorometer 110, except that the last modification (removal of the Wratten-Filters was not made).
2011.07.09 (22.00-UTC+2) Conductiviy increase	2011.07.10	Heinz Surbeck	Saturday July 9, around 22:00 (UTC+2) something has happended with the Brigerbad water composition The conductivity has nearly doubled within an hour and the gas monitor stopped working. (see Figure 30). A possible reason for the monitor program to hang is a radon counter overflow (> 65'000 counts/7min). The count rate at the last measurement (21:00 UTC+2) has been around 6'000 counts/7min. On the SED earthquake map there is an about magnitude 2 red spot near St.Niklaus. Unfortunately this quake is not yet in the list so I don't know when it has happened. Would be intersting if it happended at the same time as the conductivity jump at the Brigerbad spring.
Information of event	2011.07.10	Donat Fäh	This was the event at St.Niklaus (time in UTC): 2011-07-10 01:24:04 46.23 7.76 1.0 automatic 1.90 (Ml) SED St. Niklaus / Switzerland
2011.07.09 21.00-22.00 (UTC+2) Thunderstorm; blackout	2011.07.13	Heinz Surbeck	Saturday July 9 between 21:00 and 22:00 (UTC+2) a heavy thunderstorm has been over the Visp-Brig area. According to Georges Arnold from the Brigerbad spa at least one lightning has hit the ground near the spa or even directly the mechanical shop building where the monitor is located. The shock must have been quite strong as the exchange tube has been removed from its fastenings. This shock should be visible on the temporary Brigerbad seismic station, if it is still in operation. There has been no blackout, the spa pumps have turned the whole night as usual. The gas monitor control program has stopped after 21:00, probably due to the strong shaking of the PC. July 11, around 11:30 (UTC+2) I've restarted the program (PC power had to be switched off before coldstart, CTRL/ALT/DEL did not work). All is working since then. There is no sign that the PC had stopped because of a counter overflow. This would still have left increased count rates today. This has definitely not been the case. The reason for the sharp conductivity increase has probably also be the strong shaking, removing mud from the electrodes. The magnitude 1.9 quake near St.Niklaus has been at July 10, 1:30 UTC, about 5 hours later than the sharp increase in conductivity and the PC failure. I'm

			sorry, but this July 9 event has clearly not been a precursor, but has been due to a lightening. recursor would have been a wonderful birthday gift, it's tomorrow, but I'm happy anyway that nothing has been destroyed by the lightning.
Connection of tube	2011.07.13	Werner Balderer	Mr. George Arnold just reported to me that the tube transporting the water was disconnected this afternoon, but he could fix it again and now it seems the water flow works as usual.
	2011.07.13	Heinz Surbeck	I've noticed that there has been a sharp drop in radon and CO2 today and that it's resuming now. Thanks for the message. Without knowing that I would have been forced to go to the Brigerbad as soon as possible. Il will probably be at Brigerbad next Tuesday to test new stronger water pump.
2011.07.20 Tube's replacement	2011.07.24	Heinz Surbeck	July 20 I've been once more at Brigerbad. After several problems with the existing tube from the spring to the monitor(it became too soft at the high temperatures there) I've replaced it by a far stronger tube.

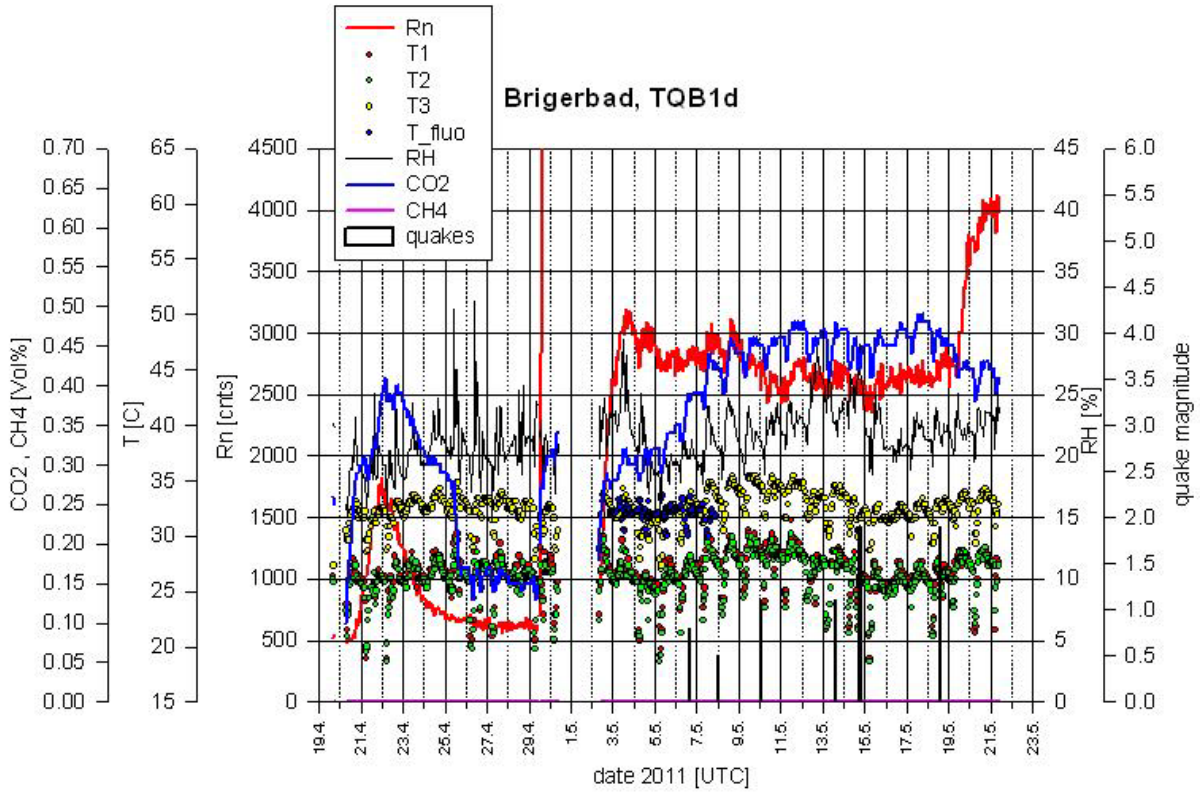
Brigerbad, TQB1d
Rn
T1
T2
T3
T_fluo
RH
CO2
CH4
quakes
CO2 , CH4 [Vol%]
T [C]
Rn [cnts]
RH [%]
quake magnitude
date 2011 [UTC]

Fig. 29

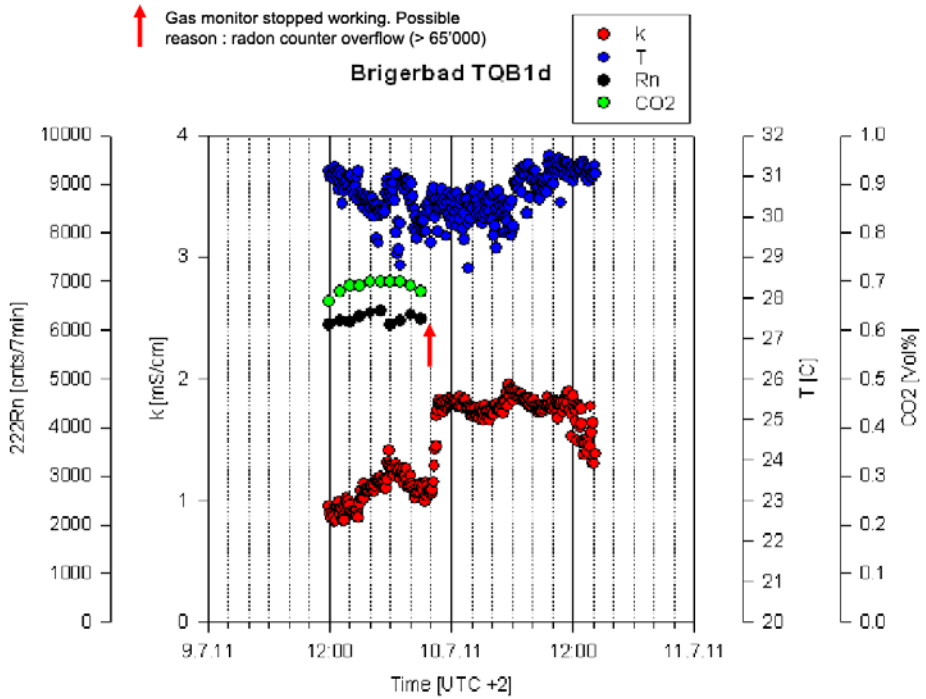
Gas monitor stopped working. Possible reason : radon counter overflow (> 65'000)
Brigerbad TQB1d
k
T
Rn
CO2
222Rn [cnts/7min]
k [mS/cm]
T [C]
CO2 [Vol%]
Time [UTC +2]
9.7.11
12:00
10.7.11
12:00
11.7.11

Fig. 30